Design, Synthesis, and Optical Characterization of a Novel, Biocompatible Azo-Polymer

Mehul Haria

Master of Science

Department of Chemistry

McGill University, Montreal

Quebec, Canada

2007 - 10 - 01

A thesis submitted to McGill University in partial fulfillment of the requirements for the degree of Master of Science

© Copyright Mehul Haria October 2007



Library and Archives Canada

Published Heritage Branch

395 Wellington Street Ottawa ON K1A 0N4 Canada Bibliothèque et Archives Canada

Direction du Patrimoine de l'édition

395, rue Wellington Ottawa ON K1A 0N4 Canada

> Your file Votre référence ISBN: 978-0-494-38401-5 Our file Notre référence ISBN: 978-0-494-38401-5

NOTICE:

The author has granted a non-exclusive license allowing Library and Archives Canada to reproduce, publish, archive, preserve, conserve, communicate to the public by telecommunication or on the Internet, loan, distribute and sell theses worldwide, for commercial or non-commercial purposes, in microform, paper, electronic and/or any other formats.

AVIS:

L'auteur a accordé une licence non exclusive permettant à la Bibliothèque et Archives Canada de reproduire, publier, archiver, sauvegarder, conserver, transmettre au public par télécommunication ou par l'Internet, prêter, distribuer et vendre des thèses partout dans le monde, à des fins commerciales ou autres, sur support microforme, papier, électronique et/ou autres formats.

The author retains copyright ownership and moral rights in this thesis. Neither the thesis nor substantial extracts from it may be printed or otherwise reproduced without the author's permission.

L'auteur conserve la propriété du droit d'auteur et des droits moraux qui protège cette thèse. Ni la thèse ni des extraits substantiels de celle-ci ne doivent être imprimés ou autrement reproduits sans son autorisation.

In compliance with the Canadian Privacy Act some supporting forms may have been removed from this thesis.

While these forms may be included in the document page count, their removal does not represent any loss of content from the thesis.

Conformément à la loi canadienne sur la protection de la vie privée, quelques formulaires secondaires ont été enlevés de cette thèse.

Bien que ces formulaires aient inclus dans la pagination, il n'y aura aucun contenu manquant.



Abstract

The goal of this thesis was to create a novel stable water-soluble azo polymer with photoswitchable properties, which was to be used as a scaffold in directing neuron growth. The new polymer, PDR2, was synthesized and extensively characterized to understand its physical and chemical properties, as well as to ascertain the structure. Characterization techniques included nuclear magnetic resonance, thermogravimetric analysis, differential scanning calorimetry, absorption spectroscopy, and ellipsometry. The photoresponsive properties of the polymer were then studied by examining quantum yields and birefringence, and the variation of these properties with humidity was examined, after being deposited onto thin films using layer-by-layer self-assembly. Quantum yields were found to increase with humidity up to a maximum determined to be at approximately 30% relative humidity, and were then found to decrease with increasing humidity. This was thought to be due to a combination of factors including plasticization and the formation of water clusters. Birefringence experiments revealed that the thin films did not produce a stable birefringence state. Many factors, including low azo content in the polymer, interaction with polymer side groups, and the mobility of polyelectrolyte multilayers were thought to contribute to these results.

Abrégé

Le but de cette thèse était de créer un nouveau polymère stable d'azobenzene avec des propriétés photo-sensitives et qui est soluble dans l'eau. Ce polymère est destiné à être utilisé comme guide directionnel dans la croissance des neurones. Le polymère, PDR2, a été synthétisé et largement caractérisé afin de mieux comprendre ses propriétés physiques et chimiques, ainsi que sa structure. Les techniques utilisées impliquent la résonance magnétique nucléaire, l'analyse thermogravimétrique, l'analyse calorimétrique à compensation de puissance, la spectroscopie d'absorption, et l'ellipsométrie. L'étude des propriétés photo-sensitives du polymère a débuté par l'examen du rendement quantique et de sa biréfringence. Les variations des ces propriétés en fonction de l'humidité ont été examinées sur un film de polymère déposé sur une lame en utilisant la technique d'auto-assemblage de couches minces superposées. Le rendement quantique augmentait avec le niveau d'humidité jusqu'à un maximum d'environ 30% d'humidité relative, puis commençait à diminuer si le niveau d'humidité continuait d'augmenter. Ces observations pouvaient résulter d'une combinaison de facteurs dont une possible plastification et la formation de micelles d'eau. Les expériences sur la biréfringence ont révélé que les couches ne produisent pas une biréfringence stable. Plusieurs facteurs, notamment moins de groupements azoïques au sein du polymère, l'interaction avec d'autres groupements contenus dans la chaîne, et la mobilité des couches polélectrolytes multiples semblent contribuer à ces résultats.

Acknowledgements

First and foremost, I would like that thank my supervisor, Dr. Christopher Barrett for the opportunity to work in his lab. His enthusiasm for science was contagious, and his support, patience, and guidance will always be appreciated.

I am very grateful to the members in the Barrett lab, past and present who have helped me and made it enjoyable to come into the lab everyday to work. Oleh and Kevin, it was a pleasure to work with both of you, and you both really helped me get under way before you left. Annie and Peter, you have both been so friendly and easy to work with in the lab and I thank you for your help and support.

There are also various other people at Otto Maass and Montreal who have helped, and I would like to thank the members of the Perepichka and Gleason groups who helped with the synthesis, and Emily for usually going well out of her way to help me out on basically anything.

There are many people in Montreal who made it so much easier to come here, and who helped make this one of the best experiences of my life. Hitesh and Blythe, I could not ask for better roommates. To everyone else, Chris Godbout, Jason, Ned, Patrick, Andrew, Chris McQuinn and Jess, you guys were the main reason why my time in Montreal was so amazing, and I truly value all of your friendship.

Gloria, you have always been there for me for everything. You have been so patient and supportive and understanding for these past few years, and you truly are an incredible person.

I have been blessed with such an amazing and caring family. Mom and Dad, you have never stopped believing in me, and I appreciate the sacrifices you have made for me. Your support and understanding has always made it easier. Finally, my brother Samir, you have shown what true courage and what true strength actually are. You have shown how to deal with adversity, without fear, but with hope and spirit and the will to never give up. You are and always will be a source of inspiration to me.

Table of Contents

Abstract	i
Acknowledgements	ili
Table of Contents	V
List of Tables	vii
List of Figures	vi
Chapter 1 Introduction	1
1.1 Background	
1.2 Azobenzene	4 8
1.3 Azobenzene Polymers	12
1.4 Polyelectrolyte Multilayers	14
1.5 Birefringence	16
1.6 Quantum Yields	17
1.7 Scope of the Thesis	21
References	
Chapter 2 Synthesis and Characterization of PDR2	31
2.1 Introduction	31
2.2 Materials	35
2.3 Synthesis of PDR2 2.3.1 - Forming the Amide from DR1 2.3.2 Formation of Poly(acyl) Chloride	35
2.4 Polymer Characterization 2.4.1 Thermogravimetric Analysis 2.4.2 Differential Scanning Calorimetry	39
2.4.2 Differential Scanning Calorimetry	

2.4.4 Ellipsometry	45
2.4.5 Nuclear Magnetic Resonance	
2.4.6 Gel Permeation Chromatography	
References	50
Chapter 3 Effect of Humidity on Quantum Yields and Birefringence	51
3.1 Introduction	51
3.2 Quantum Yields	52
3.3 Birefringence	61
3.4 Optical Setup – Quantum Yields	63
3.4.1 Optical Configuration for Birefringence Measurements	65
3.5 Experimental Procedure	66
3.6 Results and Discussion – Quantum Yields	67
3.6.1 Discussion and Results - Birefringence	
3.7 References	83
Supporting Information	85
Chapter 4 Conclusions and Future Work	88
4.1 Conclusions	88
4.2 Future Work	90

List of Tables

Table 3.1: Birefringence parameters of PDR2 with increasing humidity

List of Figures

- Figure 1.1: Structure of trans and cis azobenzene
- Figure 1.2: Absorption spectra of the three different classes of azobenzenes
- Figure 1.3: A simple state model for azobenzene isomerization
- Figure 1.4: Isomerization of Poly Disperse Red 1
- Figure 1.5: Schematic of layer-by-layer self-assembly
- Figure 2.1: NMR spectrum of PDR1A after hydrolysis
- Figure 2.2: Outline of the process used to synthesize Poly Disperse Red 2
- Figure 2.3: NMR spectrum of a methyl sulfate functionalized Disperse Red 1
- Figure 2.4: Thermogravimetric analysis of PDR2
- Figure 2.5: Differential Scanning Calorimetry of PDR2
- Figure 2.6: Absorption spectra of PDR2 on thin films and in solution
- Figure 2.7: Determination of PDR2 extinction coefficient
- Figure 2.8: NMR spectrum of PDR2
- Figure 3.1: Pump-probe experiments for PDR2 at increasing irradiation intensities
- Figure 3.2: Rau plot of a 15-layer PDR2 sample at 43% relative humidity
- Figure 3.3: Schematic of photo-orientation of azo chromophores

- Figure 3.4: Optical setup used for measuring quantum yields
- Figure 3.5: Optical setup used to measure birefringence
- Figure 3.6: Variation of quantum yields with increasing humidity
- Figure 3.7: Change in Δ -max with humidity
- Figure 3.8: Typical pump-probe curve for PDR2
- Figure 3.9: Relaxation curve of PDR2
- Figure 3.10: Influence of humidity on relaxation rates
- Figure 3.11: Standard birefringence curve
- Figure 3.12: Birefringence curve of PDR2 at 60% relative humidity
- Figure 3.13: Biexponential fit for the rise and decay of PDR2 birefringence
- Figure 3.14: Structures of NBEM and styrene
- Figure 3.15: Variation of birefringence relaxation times with humidity
- Figure 3.1S: Variation in quantum yields with humidity for a 10-layer sample
- Figure 3.2S: Change in Δ -max with humidity for all three sets of experiments

Chapter 1

Introduction

1.1 Background

Controlling cell responses to an implantable material is essential to tissue engineering. Because the surface of the material is in direct contact with cells, the chemical and topographical properties may play an essential role [1]. Topographical effects on cell behaviour have been noticed since the turn of last century on nerve cells cultured on cover slips [2]. Earlier studies on the effect of substrate topography on cell behaviour lacked precise control of the structure, however, with the advent of micro- and nano- fabrication, well-defined and precisely controlled features have been produced on materials. With this technology, it has been shown that shape, dimension, and distribution of the features can all impact cell behaviour [3,4].

Neuronal connections form during embryonic development when neurons send out axons. These are led by the growth cone, which migrates through the embryonic environment to its targeted synapses [5]. Studies of developing axonal targets have shown that axons extend to their targets in a stereotyped and directed manner by detecting a variety of attractive and repulsive molecular guidance cues presented by cells in the environment [6,7]. Various families of guidance cues, either attractive or repulsive, have been identified; as well, certain growth factors have been implicated in axon guidance [6-10]. While the complete mechanism of how neuron

cells grow has proved to be too complex to be fully understood so far, it is agreed upon that it is the spatial gradients of these axon guidance molecules are detected by the growth cone and provide directional information [11-15].

Various forms of gradients, from concentration to electrical, have been formed and modified in many ways, but one fascinating method to form and modify gradients uses light to control optically active materials. Optical tools have been developed in the microelectronics industry for use in light patterning and have achieved remarkable control over material properties. With the advancement of optical tools and technology, it has become possible to investigate patterning techniques that take advantage of this visible-light lithographic infrastructure [16]. Photo-responsive materials, when irradiated, exhibit different properties than in the non-irradiated state, which can be used to locally modify material properties. Exploiting these properties can allow for changes in the topographical features, and form gradients, which can both be modified for use in neuron cell growth. One class of extensively studies optically active materials is based on the azobenzene structure.

1.2 Azobenzene

Azobenzene is an aromatic molecule characterized by an azo linkage connecting two phenyl rings. Commonly, the term 'azobenzene' or 'azo' refers to the general azobenzene structure, though different substituents may be added, which can change the physical and chemical properties of the azos. All azobenzenes have a

strong electronic absorption due to the highly conjugated π -system. The absorption spectrum can be tailored, through substituents, to lie anywhere from the ultraviolet to the visible-red region.

$$\frac{h\nu}{h\nu',\Delta}$$

Figure 1.1 The energetically favourable *trans* azobenzene can be photoisomerized to *cis*, which can revert back either through absorption in the visible spectra, or thermally.

One of the most unique and interesting characteristics about azobenzenes is their efficient and fully reversible photoisomerization. Azobenzenes are thermally stable in the *trans* state and have a metastable *cis* configuration. The azo chromophore can convert from the *trans* to *cis* form through absorption of a photon. Most azobenzenes can then be optically isomerized back to the *trans* form with visible light or they can also thermally relax back to the more stable *trans* state.

1.2.1 Azobenzene Chromophores

Azobenzenes can be separated into three different classes dependent on the nature of the substituents, as well described by Rau [17]. They are defined by the energetic ordering of their $n \to \pi^*$ and $\pi \to \pi^*$ electronic states and consist of: azobenzene type molecules, aminoazobenzene-type molecules, and pseudo-stilbenes.

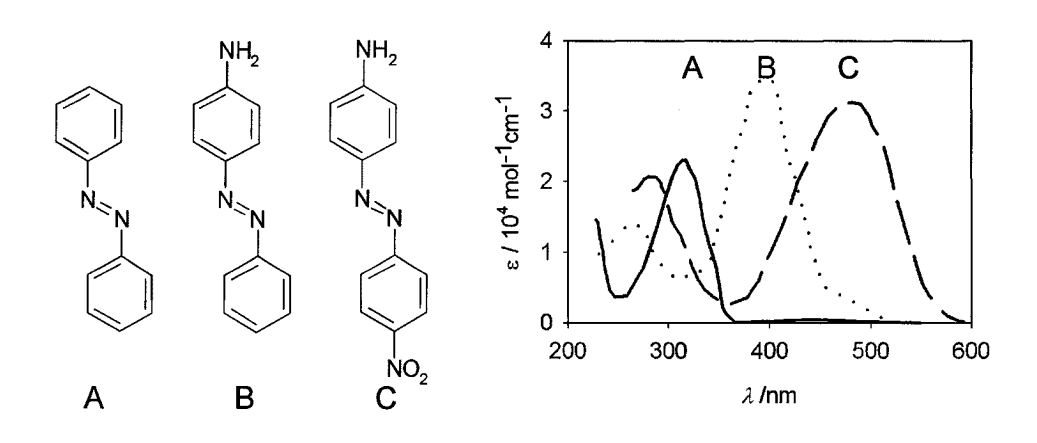


Figure 1.2 The absorption spectra of the three classes of azobenzenes a) azobenzenes b) stilbenes c) pseudo-stilbenes.

The azobenzene class has a low-lying $n \to \pi^*$ transition band. Though symmetry forbidden, the transition is intense due to non-planar distortions and vibrational couplings. The *cis* form, however, has a symmetry allowed $n \to \pi^*$ transition, but demonstrates a low intensity due to little spatial overlap between the $n \to \pi^*$ molecular orbitals. The $n \to \pi^*$ transition is intense in the *trans* isomer, and

decreases in intensity in the *cis* form. The aminoazobenzene type molecules are characterized spectroscopically by a close proximity of the $n \to \pi^*$ and $\pi \to \pi^*$ bands, due to the presence of an electron donating group like NH₂ on the ortho- or para- position of the ring. Azobenzene chromophores classified under the pseudostilbene class have the electronic states reversed due to the presence of electron-donating and electron-withdrawing groups on the 4 and 4' positions of the phenyl ring [18].

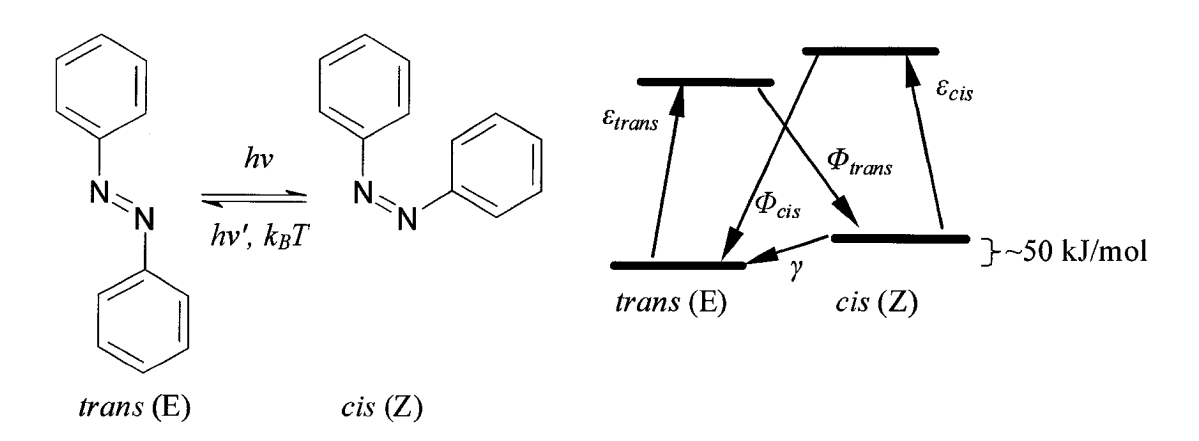


Figure 1.3 a) The photochemical *trans* to *cis* isomerization and relaxation back to the thermally stable *trans* state. b) A simple state model for azobenzenes. The *trans* and *cis* extinction coefficients are denoted ε_{trans} and ε_{cis} . The quantum yields are denoted by Φ , and γ is the thermal relaxation.

The distinct absorption spectra for the three classes of azobenzenes account for their prominent colours of yellow, orange, and red, respectively, although the addition of substituents may lead to changes in spectroscopic character. While azobenzenes are insensitive to solvent polarity, the position of the absorption bands on solvent polarity is more expressed in aminoazobenzene type molecules.

The different characteristics of the photoisomerization of azobenzene depend strongly on the degree of substitution on the phenyl rings. Most importantly, the wavelength of the light required to induce isomerization varies significantly from one spectral class to another. This effect is of great practicality because the synthesis of the azobenzene systems can be tuned to correspond to the requirements of a particular application. Azobenzene chromophores can be oriented using polarized light via a statistical selection process [19]. When probed with polarized light, the azo thin films show an increased absorbance and refractive index in a particular direction, which represents birefringence, anisotropy in the refractive index, and dichroic properties, which is anisotropy in the absorption spectra. [20]. Azobenzenes preferentially absorb light polarized along their transition dipole axis, which is the long axis of the azo molecule. The probability of absorption varies as $\cos^2 \Phi$, where Φ is the angle between the light polarization and azo dipole axis. Causing those azos oriented along the polarization of the light to absorb, and conversely, those oriented against the light polarization will not. The reorientation in the direction perpendicular to light polarization is known as cooperative motion, and is common in ordered materials [16]. For a given initial angular distribution of chromophores, many azos will absorb and convert into the cis form, after which they will revert thermally to the trans form

with a new random orientation. Those chromophores that fall perpendicular to the light polarization will no longer isomerize and reorient, reducing the number of chromophores aligned with the light polarization, but increasing the number of chromophores aligned perpendicularly. This statistical reorientation is fast and is responsible for the strong birefringence and dichroism.

The orientation due to polarized light is reversible. The direction can be modified by using a new polarization direction for the irradiating light. Circularly polarized light will randomize the chromophore orientations. There is, however, a competing effect, as the chromophores also show preferential alignment along the axis of incoming light. It is unavoidable that the chromophores will eventually build up, aligning along the irradiation axis [21]. When probed with polarized light, the azo thin films show an increased absorbance and refractive index in a particular direction, which represents birefringent and dichroic properties [22]. This induced dichroism and birefringence is only possible because the azobenzenes are mobile and respond to light by a motion. One would assume that this could only be possible in liquid crystalline systems because of the relative freedom that the chromophores have in such systems. However, investigations have indicated that azobenzenes move in more rigid polymer systems and that this motion is specific to azobenzenes and not to the hosting systems [23,24].

The versatility of azo systems has allowed them to be used for various situations, ranging from their original uses as dyes [25,26], to photoswitches [27], and

even photoprobes [28,29]. The birefringent properties [24] of azos also allowed for the possibility of data storage [30,31].

1.2.2 Azobenzene Isomerization

Some of the most intriguing and interesting applications of azobenzenes are due to the clean and efficient photoisomerization about the azo bond. The photoisomerization is completely reversible and free from side reactions. The *trans* isomer of a simple azobenzene is more stable by about 50kJ/mol [32,33] and the energy barrier to the photo-excited state is approximately 200kJ/mol [34], though that is dependent on the type of chromophore. In the dark, most azobenzene molecules will be in the *trans* configuration, and will isomerize upon absorption of a photon whose energy corresponds to a region in the *trans* absorption band, with isomerization occurring on the picosecond time scale [35,36,37]. A second wavelength of light results in the back conversion. In some cases, bulky substituents may inhibit the $cis \rightarrow trans$ relaxation process, allowing the azobenzene to remain in the cis state for days [38]. The cis to trans relaxation can be prevented through either adsorption to a surface [39] or adding constrained substituents [40].

Studies have demonstrated that *cis*-azobenzene molecules obtained from the transformation of the planar *trans* form have globular geometry with the phenyl rings twisted perpendicular to the plane [41]. The distance between the 4 and 4 positions of the *trans* azobenzene is 1.0 nm and the same distance is 0.56nm for the *cis*-

azobenzene [42]. The dipole moment is increased upon *trans-cis* photoisomerization from 0.5 to 3.1 Debye units.

A bulk sample of azo will achieve a photostationary state upon irradiation with a steady-state trans/cis composition based upon the competing effects of photoisomerization into the cis state and thermal relaxation back to the steady trans state. Subsequent reconversion to the cis state is also possible upon absorption of another photon. The steady-state composition is unique to each system and depends on the quantum yields for the two processes, and the thermal relaxation rate constant. Because azos are photochromic, in that their colour changes upon irradiation due to a shift in the absorption maximum, absorption spectroscopy can be used to measure the cis fraction in the steady state [43,44]. The shift in maximum wavelength absorption means that more light will pass through a thin-film sample on conversion to cis, compared to the trans configuration if irradiated at, or close to, the maximum absorption for the trans state. The difference in absorbance can then allow for the cis fraction to be measured. Under moderate irradiation, the composition of the photostationary state is predominantly cis for azobenzenes, mixed aminoazobenzenes, and predominantly trans for pseudo-stilbenes. In the dark, the cis fraction is below most detection limits and the sample is considered to be in an all trans state.

1.2.3 Mechanism of Isomerization

The photoinduced isomerization proceeds though a change in the energy and absorption intensities, and also through a change in the structure; whereas the *trans* isomer assumes a planar shape, the *cis* form adopts a three-dimensional geometry with the phenyl rings positioned at right angles of the C-N=NC plane [45].

The mechanism of isomerization is still under debate, with the two leading theories proposing either inversion or rotation. Inversion would occur with a semi-linear and hybridized transition state while the π -bond remains intact, whereas rotation would occur about the azo bond, with the rupture of the π -bond. The thermal back-relaxation is generally agreed upon to be via rotation, but both mechanisms appear viable for the photochemical isomerization [46].

Early suggestions were geared towards a rotation mechanism dominating, with minor contributions from inversion [47]. More recent experiments utilizing molecular constraints on azobenzene isomerization show support for inversion [48 – 50]. Recently, femtosecond time-resolved fluorescence suggests that inversion is the dominant process [51], as the N=N double bond is seen in the excited state. However, studies have provided evidence that the pathway is compound specific, with a nitrosubstituted azobenzene being photo-isomerized through rotation [52]. Further studies using *ab initio* calculations show that both pathways are energetically accessible, though inversion is preferred [53]. Since the difference in ground state energy between the more thermally stable *trans* and *cis* states is dependent on the type of

chromophore, both mechanisms may compete, with the environment and chromophore determining which process is preferred. Current consensus indicates that inversion is the dominant pathway for most azobenzenes [54]. This also explains how azos are able to isomerize easily, even in rigid matrices, since the inversion mechanism requires less free volume than the rotation.

The thermal isomerization follows first order kinetics in general. Hence the slope of the log of (A - A(t)) against time would give the rate constant, where A is the absorbance of the sample at infinite time (A) or at time t of the experiment (A(t)). It is important to note that the rate and extent of the isomerization depend on the spectral class of the chromophores and the local environment. In general, lifetimes of azobenzenes, aminoazobenzenes, and pseudo-stilbenes are in the order of hours, minutes, and seconds respectively, although quicker decay rates can occur in highly strained configurations. The different characteristics of azobenzene photoisomerization are largely dependent on the substituents on the phenyl rings. The maximum wavelength required to induce isomerization varies largely from one spectral class to another [55,56], which allows for azobenzene systems to be synthetically tuned to correspond to the requirements of a specific function.

1.3 Azobenzene Polymers

Azo polymers are polymers that have -N=N- groups within the polymer structure. The position of the -N=N- groups determine their broad classification as either main-chain or side-chain azo polymers. Side groups could further classify them as polyesters [57], polyamines [58], or various other groups. Azo polymers are receiving increasing attention because of their special properties and their potential applications. Many studies have been done on the trans-cis isomerization of the -N=N- groups of azo aromatic compounds in solution [59] or in the solid state [60]. Various azobenzene derivatives have been utilized as dopants [61,62] for conventional polymers to form polymer composites and change polymer properties, though it has been found that many interesting photomechanical effects do not couple to the polymer matrix in these systems. There has also been an increase in interest about azo polymers which have the azo groups covalently bound within the polymers. The influence of the polymer properties on the photochemical and thermal isomerization has been demonstrated by kinetic studies on different azo polymers [57,58,63,64] and the rate of isomerization of the azo groups attached covalently to the polymers depends on the structural properties of the polymer matrix.

Incorporating azobenzenes into polymers provides both the polymer, and the azo moiety with certain advantages. One is that the low-molecular weight azobenzene, relative to a larger polymer, gains stability and rigidity when bound to large molecules while the azos can also impart some of their photomechanical

properties to the polymer, making the polymer photoresponsive. Azo polymers can also be made advantageous by providing the azo compound with properties it would otherwise not have, such as solubility in water. Azos are typically insoluble in water, limiting their use in biological applications. However, forming a polymer with a water-soluble backbone, and small amounts of azo, would allow for the polymer, and hence, the azo, to be water-soluble. Attempts have been made at creating water-soluble azo polymers using this philosophy, however, rapid degradation in water has limited their effectiveness [65,66].

Figure 1.4 Poly Disperse Red 1-co-poly(acrylic acid) (PDR1A) is an extensively studies poly azo. The photochemical properties of DR1 remain intact in the polymer chain.

There are two main strategies to synthesizing polymer-containing azobenzenes. One approach involves the polymerization of monomers already containing the azobenzene moiety [67,68]. This method, known as direct polymerization, is useful because it provides control over the sequence distribution in the polymer. The second approach involves chemically modifying preformed polymers [69 – 71]. One major advantage to this method is the commercially available starting materials, though attaining the final product may still require a multi-step approach. The azobenzene groups can be introduced into either the main chain of the polymers or on side chains.

1.4 Polyelectrolyte Multilayers

Polymers can be deposited on a solid substrate by various techniques, however, a new facile and versatile preparation technique, layer-by-layer electrostatic self-assembly, is frequently used [72 – 74]. Layer by layer adsorption is the constructive deposition of molecular layers onto surfaces of solid support by alternating exposure to positively and negatively charged species (Figure 5). Each exposure deposits a consistent amount of material and reverses the charge on the surfaces, allowing the next layer to be added. This method has been called self-assembly layer-by-layer adsorption (SALBL) since the driving mechanism is the self-assembly.



Figure 1.5: In layer-by-layer self-assembly (LBLSA), the charge at the surface alternates by layer deposition using dilute polyanion and polycation solutions. This procedure can be repeated for as many layers as are required.

These polyelectrolyte multilayers are easy to prepare and tunable by adjusting such parameters as ionic strength [75,76] or pH [77 – 79]. The thickness [76], permeability [80], and density [81] can also be adjusted, providing different properties. The main requirement for a successful LBL is the presence of interactions between the different layers. This is where the versatility of the method is extremely important, as a wide range of intermolecular interactions, such as hydrogen bonding [82], Van der Waals [83], or covalent chemistry [84], can be used to form the films. The electrostatic attraction between oppositely charged species has the advantage of being highly stable, which is why LBL is most commonly used. The layered species can be controlled in the direction normal to the substrate, which allows for good positioning of the individual layers and enables the formation of nanostructured films. Also, this technique is not limited to flat surfaces. Any geometry that can be immersed in the solution is suitable. Aside from poly-azo films, a wide variety of

materials, such as natural proteins [85], colloids [86], dendrimers [87], and semiconductor nanoparticles [88] have all been layered through this method.

1.5 Birefringence

When azo chromophores are irradiated with light polarized in the y-direction, a net alignment of chromophores in the x-direction is observed, and vice-versa. Consequently, the refractive index probed in the x direction, n_x , will measure the corresponding azos along the long axis and will be larger than the refractive index in the y-axis. Birefringence is the anisotropy in refractive index: $\Delta n = |n_x - n_y|$. Photoalignment in azobenzene systems has been shown to achieve extremely high values of Δn , up to 0.3 - 0.5 at ~633nm [89,90]. The high birefringence values can be obtained far outside the azo absorption band, which is extremely important because it allows the birefringence to be measured and utilized without disrupting the azo chromophores. Subsequent irradiation of linearly polarized azo systems with circularly polarized light can bring an in-plane isotropic state ($n_x = n_y$), and a fully isotropic state can be obtained by heating above the glass transition temperature. The anisotropy of the *cis* population during irradiation can be measured in some systems where it is found that, as with *trans*, there is an enrichment perpendicular to the irradiation polarization [91,92].

The birefringence can be written and erased hundreds of times without consequence, making it an important and well studied area of azo systems [93].

Amorphous polymer systems with high glass transition temperatures exhibit good stability of any induced orientation, though some order is lost upon heating, and full isotropy can be restored upon heating above the glass transition temperature. A short spacer between the chromophore and polymer backbone slows the growth of birefringence, yet promotes stability, due to hindered motion. The ease and repeatability of birefringence in azo systems allows for a number of unique applications. They can create polarization filters, which can be used to separate right-handed from left-handed circularly polarized light [94]. It can serves as a waveguide by patterning the refractive index contrast into a line [95,96]. Birefringence gratings can also be formed by illuminating the azo samples with a spatially varying light pattern, which is the basis of holography [97 – 99]. Holography is two interfering coherent beams creating a spatially varying light pattern, which is encoded into the material. Illumination of the material with one of the beams produces the other encoded beam through diffraction [100].

1.6 Quantum Yields

One of the great advantages of dye-doped or dye-functionalized polymers is their ability to form thin films for optics. Another advantage is due to the photochemical properties of the dye or polymer, which allows transformation by visible, or UV light, to create interesting physical or physiochemical changes of the film, such as refractive index variations [101,102]. The quantum yield then, is

important in helping to determine the mechanisms by which the photochemical changes occur.

The quantum yield of a substance is the change that occurs per absorbed photon, in effect, making the quantum yield the efficiency with which absorbed light produces some effect. A system in which a change is caused by every absorbed photon would have a quantum yield of 1, but since for most systems, not all photons are absorbed productively, quantum yields usually range from 0 to 1. Systems have been identified with quantum yields greater than 1. In these cases, an absorption of a photon leads to a series of events, each of which is considered a change in the system. To calculate the quantum yield, the extinction coefficient for the cis state, among other factors, must be known. This is straightforward in a lot of cases, however, it becomes difficult in systems with temporary, or metastable, cis states, since simple absorption measurements cannot be performed [103]. Further problems arise from systems where thermal relaxation can also convert the cis form to trans, as it cannot be determined which process (irradiation, or thermal relaxation) is responsible for the isomerization during the experiments [104]. A way to resolve this is to make assumptions about the composition of the sample in the photostationary state [105]. Fischer published a method to determine the extinction coefficient of the cis state using purely spectroscopic data [106]. He used irradiation at two wavelengths and evaluated the differences of the absorbance of the sample of the pure and photostationary states. This method requires that the ratio of the quantum yields is

independent of irradiation wavelength. Although the photostationary state is dependent on the intensity of irradiation, the quantum yields are not.

Azo compounds are greatly affected by the ring substitution patterns, particularly the absorption spectra. The electron push-pull effects of pseudo-stilbenes causes the absorption bands for both cis and trans to overlap significantly, which allows a single wavelength of light to effectuate both the forward and reverse reactions, leading to a mixed stationary state and continual interconversion of the molecules. Since both trans and cis forms can be pumped by the same irradiation and interconverted, an equilibrium of the two isomers called, the photostationary state, is reached. In addition, the thermal cis-trans reactions tend to move the equilibrium in favour of the trans isomer. The first part of the experiment consists of determining the absorbance of hypothetical photostationary states of the photoreaction alone by extrapolating the pump beam intensity to infinity for various analysis and irradiation wavelengths. In the second part, these extrapolated values of the absorbances are treated by Fischer's method to determine the extinction coefficient & of the cis form. The determination of the quantum yields can than be calculated from the data. Dumont modified the ideas of Rau and Fischer [104,106] to apply to thin polymeric films, rather than solution [107]. The determination of quantum yields based on Dumont's method relies on the assumption that the equations governing the photostationary state apply equally well in thin film as in solution. With knowledge of the absorbances at a variety of photostationary states (pumped at different

wavelengths) in systems without thermal decay, Fischer's method can be used to find ε at any wavelength, indirectly plotting the electronic spectrum of the short-lived *cis* isomer. This becomes much more complicated in systems with thermal decay, as the equilibrium is moved in favour of the *trans* isomer, though this problem can be circumvented by Rau's method.

The dominant reconversion process from photogenerated cis depends on the intensity of irradiation. At low intensity, the thermal relaxation plays a larger role than cis-trans photoisomerization, and at high intensity, the photoreaction dominates. At infinite irradiation intensity, the thermal reconversion should be negligible. An estimation of infinite intensity can be determined by extrapolating the difference between A_0 and A_∞ , measured at varying intensities.

Two wavelengths with unlike absorbance values are used to provide three sets of pump/relax curves irradiating and probing either on λ -max or on the shoulder, which ensures that the quantum yields are independent of the wavelength. Measuring the amount of signal that can be induced, proportional to the concentration of *cis* isomer at various wavelengths for the three series allows an estimate of the absorbances at the photostationary state in the absence of thermal relaxation, which can then achieve the desired photochemical characterization. The only rigid guidelines for choice of wavelengths λ and λ ' are unlike extinction coefficients and excitation into the same excited state.

Quantum yields for the azobenzene molecule are on the order of 0.6 for the $trans \rightarrow cis$ photoisomerization and 0.25 for the back reaction. Aminoazobenzenes and pseudo-stilbenes isomerize very quickly and have achieved quantum yields as high as 0.7 - 0.8 [107]. Solvent is known to effect the $trans \rightarrow cis$ isomerization, and this has been shown to also affect quantum yields by increasing the $trans \rightarrow cis$ isomerization and decreasing the reverse [108]. Humidity has also been shown to have an effect on isomerization and on swelling features [109], though its effects on quantum yields have yet to be explored.

1.7 Scope of the Thesis

The goal of this thesis is to construct a polymer with the characteristics suitable for use as a substrate in neuron growth, namely a water-soluble polymer that can provide quick and efficient optical responses and is cell compatible. Water-soluble azo-polymers have been previously constructed, however, their degradation in water, when incorporated into thin films has not allowed them to be suitable for the purposes of this project. It is, therefore, imperative that the newly constructed molecule withstands hydrolysis for long periods of time. Furthermore, this molecule will be fully characterized and will provide the starting point for this project to further develop. Also, the quantum yields will be determined and specifically what role, if any, humidity plays in quantum yields. Finally, birefringence experiments will be carried out, in order to better understand this, and similar polymeric compounds.

The first chapter has been an overview of the general characteristics and applications of azo-based compounds, with more emphasis on their use in polymeric systems and thin films. It has also shown how azo compounds show potential as a scaffolding material for use in neurological experiments. The second chapter will illustrate the rational behind choosing a suitable molecule, along with the synthesis and characterization. The third chapter will show optical characterization, by determining quantum yields, and how they are affected by humidity. This is done with a complex laser set-up, and using purely spectroscopic data to circumvent attaining the metastable *cis* isomer. Relaxation times, imperative to quantum yield calculations, were also determined, and the theory and method behind relaxation times is also discussed here. A humidity cell was constructed solely for the purpose of attaining constant humidity, which could be tuned to range from 3% to 98% relative humidity. The fourth chapter will discuss the principles of birefringence and the data obtained from the newly constructed polymer. Finally, a fourth chapter will consist of concluding remarks and future considerations.

References

- [1] Tan, J.; Saltzman, M. W. Biomaterials 2002, 23, 3215.
- [2] Harrison, R. G. Anat. Rec. 1912, 6, 181.
- [3] Curtis, A.; Wilkinson, C. Biomaterials 1997, 18, 1573.
- [4] Brunette, D.M.; Chehroudi, B. J. Biomech. Eng 1999, 121, 49.
- [5] Tessier-Lavigne M.; Charron, F. Development 2005, 132, 2251.
- [6] Tessier-Lavigne, M.; Goodman, C.S. Science 1996, 274, 1123.
- [7] Dickson, B.J. Science 2002, 298, 1959.
- [8] Ebens, A.; Brose, K.; Leonardo, E. D.; Hanson, M.G.; Bladt, F.; Birchmeier, C.;
- Barres, B.A; Tessier-Lavigne, M. Neuron 1996, 17, 1157.
- [9] O'Connor, R.; Tessier-Lavigne, M. Neruon 1999, 24, 165.
- [10] Tucker, K.L.; Meyer, M.; Barde, Y.A. J. Neurosci. 2001, 4, 29.
- [11] Zheng, M.; Kuffler, D.B. J. Neurobiol. 2000, 42, 212.
- [12] Hayden, P.G.; McCobb, D.P.; Kater, S.B. Science 1984, 226, 561.
- [13] Mattson, M.P.; Dou, P.; Kater, S.B. J. Neurosci. 1988, 8, 2087.
- [14] Isbister, C.M.; Mackenzie, P.J.; To, C.W.K.; O'Connor, P.O. J. Neurosci. 2003, 23, 193.
- [15] Goodhill, G.J.; Baier, H. Neural Computation 1998, 10, 521.
- [16] Natansohn, A.; Rochon, P. Chem. Rev. 2002, 102, 4139.
- [17] Rau, H. "Photochemistry and Photophysics" (J. Rebek, Ed.), Vol. 2, pp. 119 –
- 141, CRC Press, Boca Raton, FL, 1990.

- [18] Rau, H. Ber. Bunsen-Ges. 1968, 72, 408.
- [19] Ichimura, K. Chem. Rev. 2000, 100, 1847.
- [20] Torodov, T.; Nikolova, L.; Tomova, N. Appl. Opt. 1984, 23, 4309.
- [21] Han, M.; Ichimura, K. *Macromolecules*, **2001**, *34*, 82.
- [22] Rochon, P.; Gosselin, J.; Natansohn, A.; Xie, S. Macromolecules 1992, 25, 2268.
- [23] Rochon, P.; Gosselin, J.; Natansohn, A.; Xie, S. Appl. Phys. Lett. 1992, 60, 4.
- [24] Zollinger, H. "Azo and Diazo Chemistry." Interscience Publishers, New York, 1961.
- [25] Zollinger, "Colour Chemistry, Synthesis, Properties, and Applications of Organic Dyes." VCH, Weinheim, 1987.
- [26] Barley, S.H.; Gilbert, A.; Mitchell, G.R. J. Mater. Chem. 1991, 1, 481.
- [27] Mermut, O.; Barrett, C.J. Analyst (Cambridge, U.K.) 2001, 126, 1861.
- [28] Uznanski, P.; Percherz, J. J. Appl. Polym. Sci. 2002, 86, 1459.
- [29] Dhanabalan, A.; Dos Santos, Jr.; D.S.; Mendonca, C.R.; Misoguti, L.; Balogh,
- D.T.; Giacometti, J.A.; Zilio, S.C.; Oliveira, Jr, O.N. Langmuir 1999, 15, 4560.
- [30] Hagen, R.; Bieringer, T. Adv. Mater. 2001, 13, 1805.
- [31] Ramanujam, P.S.; Hvilsted, S.; Ujhelyi, F.; Koppa, P.; Lorincz, E.; Erdei, G.; Szarvas, G. Synth. Met. 2001, 124, 145.
- [32] Schulze, F.W.; Petrick, H.J.; Cammenga, H.K.; Klinge, Z. Physiol. Chem. 1977, 107, 1.

- [33] Mita, I.; Horie, K.; Hirao, K. Macromolecules 1989, 22, 558.
- [34] Monti, S.; Orlandi, G.; Palmieri, P. Chem. Phys. 1982, 71, 87.
- [35] Kobayashi, T.; Degenkolb, E.O.; Rentzepis, P.M. J. Phys. Chem. 1979, 83, 2431.
- [36] Lednev, I.K.; Ye, T.-Q.; Hester, E.; Moore, J.N. J. Phys. Chem. 1996, 100, 13338.
- [37] Fukino, T.; Arzhanstev, S.Y.; Tahara, T. J. Phys. Chem. A. 2001, 105, 8123.
- [38] Shirota, Y.; Moriwaki, K.; Yoshikawa, S. Ujike, T.; Nakano, H. *J. Mater. Chem.* **1998**, *8*, 2579.
- [39] Kerzhner, B.K.; Kofanov, V.I.; Vrubel, T.L. Zh. Obshch. Khim. 1983, 53, 2303.
- [40] Funke, U.; Gruetzmacher, H.F. Tetrahedron 1987, 43, 3787.
- [41] Naito, T.; Horie, K.; Mita, I. Polym. J. 1991, 23, 809.
- [42] Delang, J.J.; Robertson, J.M.; Woodward, I. Proc. R. Soc. London, Sect. A, 1939, 171, 398.
- [43] Fisher, E. J. Phys. Chem. 1967, 71, 3704.
- [44] Rau, H.; Greiner, G.; Gauglitz.; Meier, H.; J. Phys. Chem. 1990, 94, 6523.
- [45] Naito, T.; Horie, K.; Mita, I. Polym. J. 1991, 23, 809.
- [46] Xie, S.; Natansohn, A.; Rochon, P. Chem. Mater. 1993, 5, 403.
- [47] Ross, D.L.; Blanc, J. *Photochromism*, Brown, G.H. Ed.; Interscience Publishers: New York, 1971.
- [48] Gegion, D.; Muszkat, K.A.; Fisher, E. J. Am. Chem. Soc. 1968, 90, 390.
- [49] Naito, T.; Horie, K.; Mita, I. *Macromolecules* **1991**, *24*, 2907.

- [50] Altomare A.; Ciardelli, F.; Tirelli, N.; Solaro, R. *Macromolecules* **1997**, *30*, 1298.
- [51] Fujino, T.; Arzhanstev, S.Y.; Tahara, T. J. Phys. Chem. A 2001, 105, 8213.
- [52] Ho. C.-H.; Yang, K.-N.; Lee, S.-N. J. Polym. Sci., Part A: Polym. Chem. 2001, 39, 2296.
- [53] Angeli, C.; Cimiraglia, R.; Hofmann, H.-J. Chem. Phys. Lett. 1996, 259, 276.
- [54] Ikeda, T.; Tsutsumi, O. Science 1995, 268, 1873.
- [55] Smets, G. Adv. Polym. Sci. 1983, 50, 17.
- [56] Williams, J. L.R.; Daly, R.C. Prog. Polym. Sci. 1977, 5, 61.
- [57] Anderle, K.; Birenheide, R.; Eich, M.; Wendroff, J.H. Macromol. Rapid. Commun. 1989, 10, 477.
- [58] Angolini, F.; Gay, F.P. Macromolecules 1970, 3, 349.
- [59] Paik, C.S.; Morawetz, H. Macromolecules 1972, 5, 171.
- [60] Barrett, C.; Natansohn, A.; Rochon, P. Chem. Mater. 1995, 7, 899.
- [61] Birabassov, R.; Landraud, N.; Galstyan, T.V.; Ritcey, A.; Bazuin, C.G.; Rahem,T. Appl. Opt. 1998, 37, 8264.
- [62] Labarthet, F.L.; Buffeteau, T.; Sourisseau, C. J. Phys. Chem. B 1998, 102, 2654.
- [63] Mekelburger, H.B.; Rissanen, K.; Voegtle, F. Chem. Ber. 1993, 126, 1161.
- [64] Junge, D.M.; McGrath, D.V. Chem Commun. 1997, 857.
- [65] Ahmad, N.M.; Barrett, C.J. Polymeric Materials Science and Engineering 2001, 85, 607.

- [66] Ahmad, N.M.; Barrett, C.J. Polymeric Materials Science and Engineering Preprints 2006, 94, 753.
- [67] Ho, M.S.; Barrett, C.; Paterson, J; Esteghamatian, M.; Natansohn, A.; Rochon, P. *Macromolecules* **1996**, *29*, 4613.
- [68] Natansohn, A.; Rochon, P.; Gosselin, J.; Xie, S. Macromolecules 1992, 25, 2268.
- [69] Wang, X.; Kumar, J.; Tripathy, S.K.; Li, L.; Chen, J.-I.; Marturunkakul, S. *Macromolecules* **1997**, *30*, 219.
- [70] Wang, X.; Chen, J.-I.; Marturunkakul, S.; Li, L.; Kumar, J.; Tripathy, S.K.; *Chem. Mater.* **1997**, *9*, 45.
- [71] Wang, X.; Balasubramanian, S.; Li, L.; Jiang, X.; Sandman, D.J.; Rubner, M. F.; Kumar, J.; Tripathy, S.K. *Macromol. Rapid Commun.* **1997**, *18*, 451.
- [72] Petty, M.C. Thin Solid Films 1992 210/211, 417.
- [73] Decher, G.; Hong, J.D. Berichte der Bunsen-Gesellschaft 1991, 95, 1430.
- [74] Decher, G. Science 1997, 277, 1232.
- [75] Sukhorukov, G.B.; Schmitt, J.; Decher, G. Berichte der Bunsen-Gesellschaft 1996, 100, 1948.
- [76] Losche, M.; Schmitt, J.; Decher, G.; Bouwman, W.G.; Kjaer, K. Macromolecules, 1998, 31, 8893.
- [77] Shiratori, S.S.; Rubner, M.F. *Macromolecules* **2000**, *33*, 4213.
- [78] Chung, A.J.; Rubner, M.F. Langmuir 2002, 18, 1176.

- [79] Burke, S.E.; Barrett, C.J. Langmuir 2003, 19, 3297.
- [79] Burke, S.E.; Barrett, C.J. *Langmuir* **2003**, *19*, 3297.
- [80] Rmaile, H.H.; Schlenoff, J.B.; J. Am. Chem. Soc. 2003, 125, 6602.
- [81] Dragan, S.; Schwarz, S.; Eichhorn, K.-J.; Lunkwitz, K. Colloids, Surf. A 2003, 195, 243.
- [82] Cao, T.; Chen, J.; Yang, C.; Cao, W. Macromol. Rapid Commun. 2001, 22, 181.
- [83]Zhifei, D.; Voigt, A.; Donath, E.; Mohwald, H. Macromol. Rapid Commun. 2001, 22, 756.
- [84] Zhang, Y.; Cao, W.; Macromol. Rapid Commun. 2001, 22, 842.
- [85] Decher, G. Comprehensive Supramolecular Chemistry; Lehn, J. M. Ed.; Pergamon Press Oxford, 1996; Vol. 9, p. 507.
- [86] Caruso, F. Adv. Mater. 2001, 13, 11.
- [87] Watanabe S.: Regan, S.L. J. Am. Chem. Soc. 1994, 116, 8855.
- [88] Lvov, T.; Ariga, K.; Onda, M.; Ichinose, I.; Kunitake, T. *Langmuir* **1997**, *13*, 6195.
- [89] Natansohn, A.; Rochon, P.; Pezolet, M.; Audet, P.; Brown, D.; To, S. *Macromolecules* **1994**, *27*, 2580.
- [90] Hagen, R.; Bieringer, T. Adv. Mater. 2001, 13, 1805.
- [91] Sekkat, Z.; Wood, J.; Knoll, W. J. Phys. Chem. 1995, 99, 17226.
- [92] Buffeteau, T.; Labarthet, F.L.; Pezolet, M.; Sourisseau, C. *Macromolecules* **2001**, *34*. 7514

- [93] Holme, N.C.R.; Ramanujam, P.S.; Hvilsted, S. Opt. Lett. 1996, 21, 902.
- [94] Natansohn, A; Rochon, P. Adv Mater. 1999, 11, 1387.
- [95] Shi, Y.; Steier, W.H.; Yu, L.; Chen, M.; Dalton, L.R. Appl. Phys. Lett. 1991, 58, 1131.
- [96] Watanabe, O.; Tsuchimori, M.; Okada, A. J. Mater. Chem. 1996, 6, 1487.
- [97] Eichler, H.J.; Orlic, S.; Schulz, R.; Rubner, J. Opt. Lett. 2001, 26, 581.
- [98] Couture, J.J.A.; Lessard, R.A, Appl. Opt. 1998, 27, 3368.
- [99] Nikolova, L.; Todorov, T.; Ivanov, M.; Andruzzi, F.; Hvilsted, S.; Ramanujam, P.S. Appl. Opt. 1996, 35, 3835.
- [100] Yamamoto, T.; Ohashi, A.; Yoneyama, S.; Hasegawa, M.; Tsutsumi, O.;

Kanazawa, A.; Shiono, T.; Ikdea, T. J. Phys. Chem. B 2001, 105, 2308.

- [101] Yongquiang, S.; Steier, W.H.; Yu, L.; Chen, M.; Dalton, L.R. Appl. Phys. Lett. 1991, 58 1131.
- [102] Beeson, K.W.; Horn, K. A.; McFarland, M.; Yardley, J.T. Appl. Phys. Lett.1991, 58, 1955.
- [103] Rau, H. J. Photochem. 1984, 26, 221.
- [104] Rau, H.; Greiner, G. J. Phys. Chem. 1990, 94, 6523.
- [105] Gabor, G.; Fisher, E. J. Phys. Chem. 1971, 75, 581.
- [106] Fischer, E. J. Phys. Chem. 1967, 71, 3704.
- [107] Loucif-Saibi, R.; Nakatani, K.; Delaire, A.; Sekkat, Z.; Dumont, M. Chem. Mater. 1993, 5, 229.

[108] Bortolus, P.; Monti, S. J. Phys. Chem. 1979, 83, 648.

[109] Tanchak, O.M.; Barrett, C.J. Macromolecules 2005, 38, 10566.

Chapter 2

Synthesis and Characterization of PDR2

2.1 Introduction

The basis of azobenzene photochemistry is the reversible *trans* to *cis* isomerization, which leads to further phenomena, such as surface patterning and mass transport [1]. The versatility of azos has been an important aspect in their studies, as the various properties of azos can be tailored to meet specific goals. Tuning can be attained by changing the structure, and hence, the properties, of the polymer backbone or sidechains. It is no surprise then, that in recent years, polymers containing aromatic azo chromophores have been extensively studied leading to a vast array of uses and applications including surface relief gratings [2], optical storage [3,4], photoprobes [5], and photoswitches [6].

Our specific objective for these azo polymers was for use as a scaffold for directing neuron growth based on exploiting the differences in physical and chemical properties that arise from isomerization. This particular application had not yet been studied, due in large part to the poor solubility in water of the azo chromophores. The approach to solving this problem was to create an azo polymer with a major portion consisting of a highly water-soluble backbone to influence solubility characteristics. The desirable molecule, it was determined, was based on a well-characterized azo polymer, PDR1 (poly disperse red 1). Although it initially appeared that PDR1 would

satisfy all of the requirements for our target molecule, it was found that the polymer degraded over time in mildly acidic conditions. This was thought to be due to the ester bond, which though normally quite stable in aqueous conditions, was more susceptible to hydrolysis when coated as a thin film. Further evidence of this was seen by NMR, as the polymer showed no traces of the ester peak (Figure 2.1).

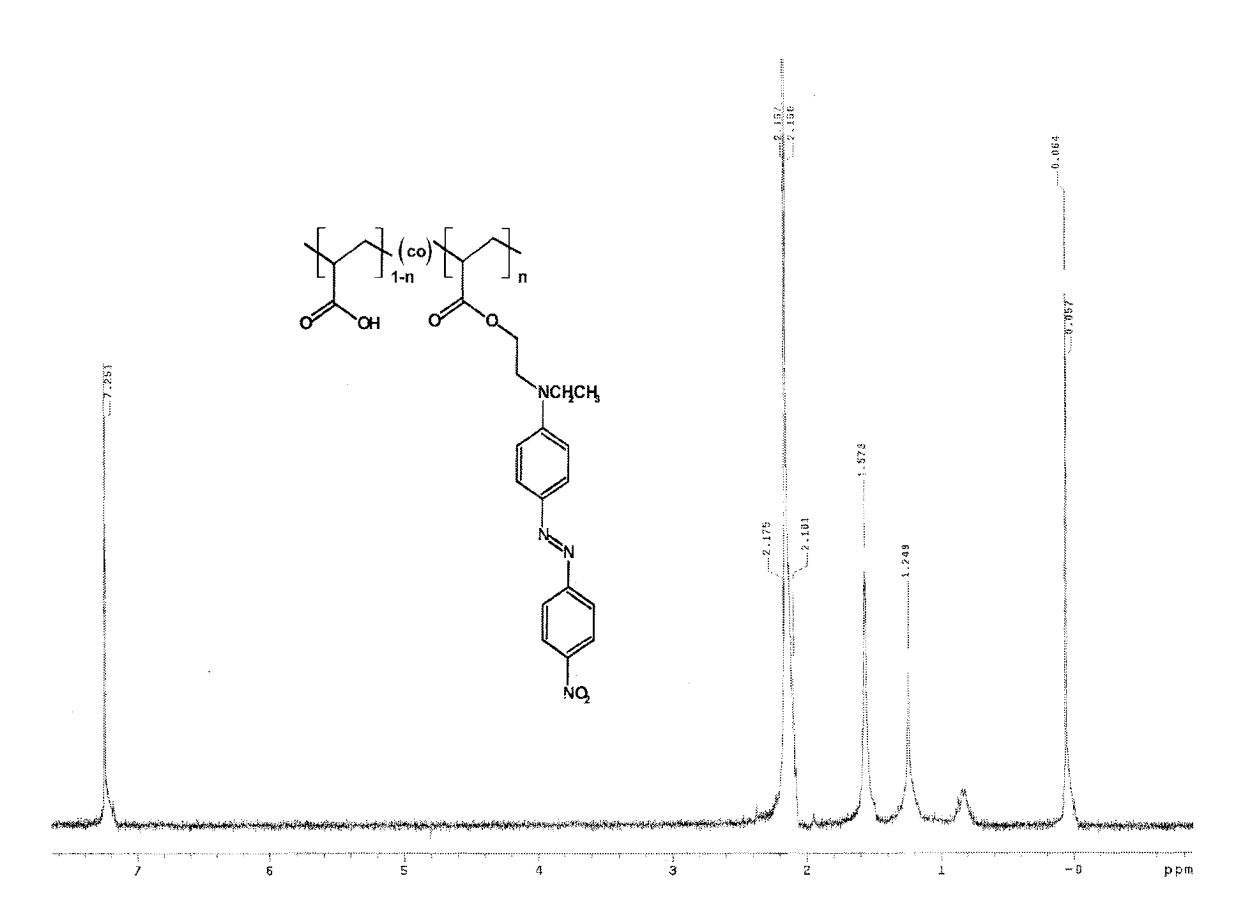


Figure 2.1 An NMR spectrum of PDR1A after it has precipitated out of solution. The ester peak at ~4.5 has disappeared, leading to the conclusion that the dye is no longer bound to the polymer. An NMR taken by a previous group member of PDR1 before being exposed to water, shows the ester peaks located ~4.5.

Thus, it was determined that a more suitable polymer would contain an amide bond in lieu of the ester bond. This new polymer was named Poly (Disperse Red 2) (PDR2).

There are two main strategies to forming poly azo compounds. The first involves functionalizing an existing polymer with the azo dye, the second is to first create a suitable monomer, then polymerize it. Both have their respective advantages and disadvantages, as discussed in Chapter 1. The former method was chosen for the basis of this synthesis, due in large part to the availability of the starting materials. In choosing this method, careful consideration of the starting materials had to be taken. Poly (acrylic acid) was eventually used as the polymer backbone due not only to its high solubility in water, but also due to its solubility in organic solvents such as THF, allowing for more options in functionalizing the polymer. The azo portion also had to be carefully constructed to allow for relatively unhindered motion during isomerization, while having the desirable push-pull properties of the pseudo-stilbene class of azobenzene still remain. The pseudo-stilbene, Disperse Red 1, contained a two-carbon spacer separating the dye portion and the attachment site to the polymer backbone, and was thus chosen as a starting point. Figure 2.2 shows a schematic of the method used to create PDR2.

Figure 2.2 - The process of making DR2. The hydroxyl group in DR1 (A) is replaced by a MESO group (B). This is then changed into an azide (C), which is finally reduced to DR2 (D). Poly(acrylic) acid (E) is made more reactive by making the acyl chloride derivative (F), then is reacted with DR2 to make the desired polymer (G).

2.2 Materials

Poly(acrylic) acid (2000 Mn Aldrich), Methane sulfonyl chloride (Aldrich), Sodium azide (Aldrich), Triphenyl phosphine (Aldrich) and 15-crown-ether (Aldrich)were all used as supplied. Tetrahydrofuran (Fisher), Dimethyl formamide(Fisher), Dimethyl chloride (Fisher), Chloroform, (Fisher), and Triethylamine (Fisher) were also all used as supplied.

2.3 Synthesis of PDR2

2.3.1 - Forming the Amide from DR1

Early attempts to merely oxidize the hydroxy group of DR1 to a carboxylic acid, then perform a coupling reaction to poly (allyl)amine hydrochloride (PAH) proved unsuccessful, as deprotonated PAH formed a sticky residue which not easily be removed from the glassware or isolated, and also due to the low yield of the carboxylic acid. Various attempts at oxidizing the hydroxyl group resulted in very low product, < 5%, with the reactant being the main result. It was then decided that an easier method might entail transforming the hydroxyl group into an amine, and reacting with the much easier to handle poly(acrylic) acid. To avoid the by-products of a coupling reaction, the poly(acrylic acid) was changed to the highly reactive poly(acyl) chloride. Replacing the hydroxy group with an amine group in DR1 was based upon published literature [7].

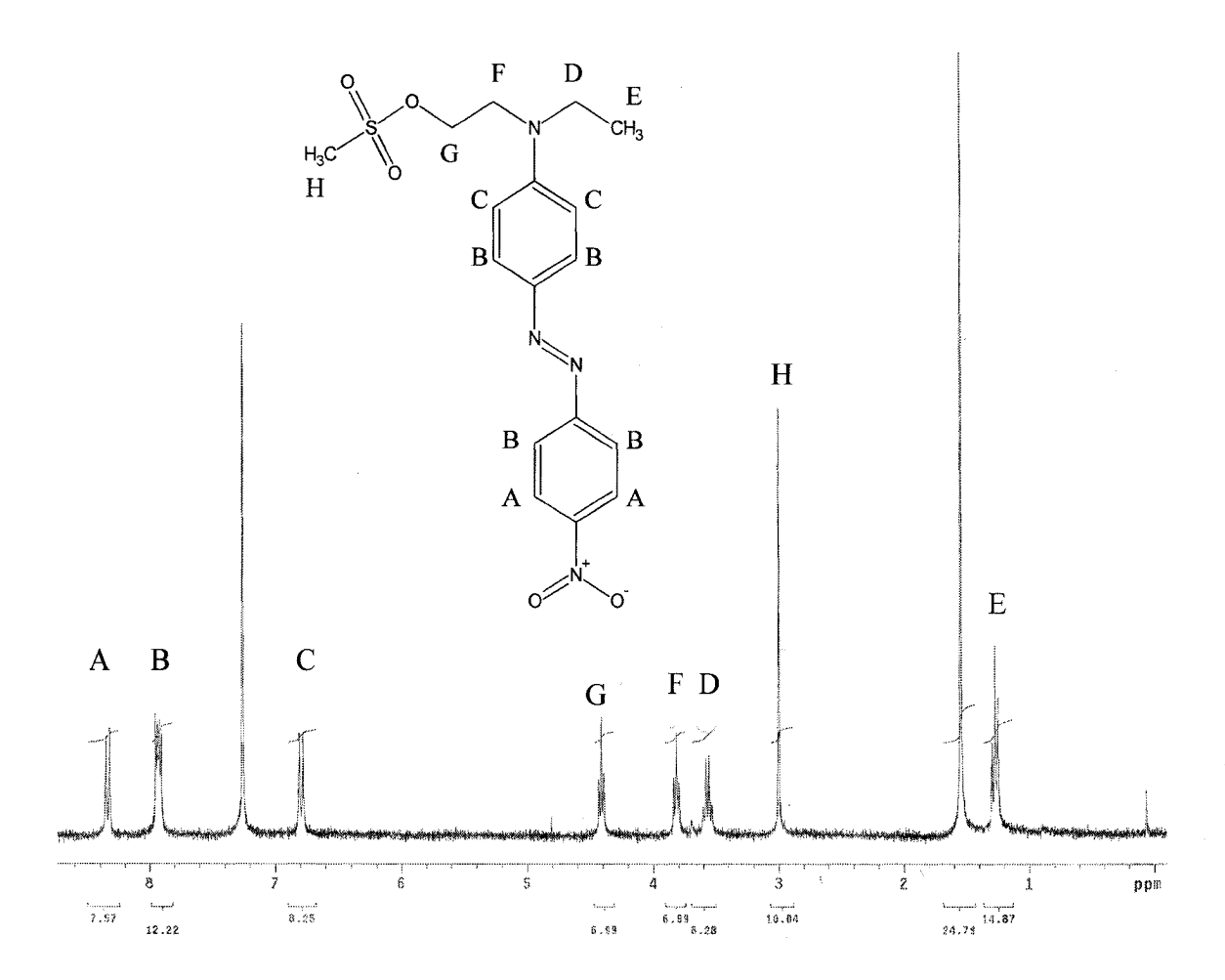


Figure 2.3 The newly functionalized dye with the hydroxy group of DR1 replaced by a methyl sulfonyl group. The assignments of the peaks are also included.

DR1 was combined with triethylamine (3:1) and methane sulfonyl chloride (2:1) in dry dichloromethane at 0°C and stirred overnight. The solution was then washed with saturated aqueous NaHCO₃ and saturated NaCl. The organic phase was then vacuumed down to dryness. Further washings with diethyl ether were required to

separate the relatively insoluble leftover DR1 with the new functionalized version. This was isolated and used for further reactions. An NMR spectrum (Figure 2.3) confirmed the presence of the newly functionalized dye. To the methyl sulfonated DR1 was added NaN₃ (6:1), and 15-crown-5 (catalytic amounts) in dry DMF and stirred overnight at room temperature. This reaction was done under argon in a dry vessel. The reaction was again washed with aqueous NaHCO₃ and saturated NaCl and vacuumed. The crude sample was then reduced with triphenylphosphine in THF with 10% water for 24 hours at room temperature with constant stirring.

2.3.2 Formation of Poly(acyl) Chloride

The poly(acrylic) acid was reacted with oxalyl chloride (1:1) in dry THF with catalytic amounts of DMF under argon and stirred for 24 hours. Combining the poly acrylic chloride and the amine-functionalized DR1 in various amounts formed the desired polymer with the amount of azo variable to specific needs. This was done in dry THF and heated for 1 hour and stirred overnight. Hexanes were used to wash the polymer of leftover TPP. Further washing was done with water, which also acted to replace the chlorine groups on the PAC with hydroxy groups, returning unreacted PAC back to PAA. The pH was adjusted to 5 – 7, using NaOH. The compound was dried by vacuum. Chloroform was then used to remove all unreacted amino DR1, leaving the pure polymer behind. Yields were low, typically about 20%.

The solubility of the purified polymer in water was low at first. This was due to the presence of hydrochloric acid resulting from the reaction between water and poly(acyl) chloride, and the result was a pH of approximately 1. After adjusting the pH with NaOH, the solubility increased noticeably. The reaction between the poly(acyl) chloride and the amine had to be performed quickly, as the poly(acyl) chloride was quick to react with water, resulting in less available sites for the reaction. Polymers were made with concentrations of azo ranging from less than 1% to 8%.

2.4 Polymer Characterization

To determine the structure of the polymer, along with its properties, several standard characterization methods were used. NMR was used for determination of the structure, and for proof that there was indeed azo attached to the polymer, rather than merely doped in the polymer matrix. It was also used to determine the purity of the polymer. Thermogravimetric analysis (TGA) was performed to determine the stability of the polymer, and differential scanning calorimetry (DSC) was used to determine the glass transition temperature, an important feature amongst azo polymers. Finally, absorption spectroscopy and ellipsometry were performed to determine the wavelength of maximum absorption and the thickness of the samples respectively. This information was further used to determine the relationship between

absorption and thickness and allow for the calculation of the absorption coefficient of the poly-azo thin film.

2.4.1 Thermogravimetric Analysis

Thermogravimetric analysis was performed on the newly formed polymer to further give insight to its physical properties and stability, and also to provide another method to determine the purity of the sample on a 220 TGA/DTA. The data revealed two different separate regions in which there was decomposition, between 60° - 135°C, and another one from 150° to 480°C. Although this resembles the results typical of a co-block polymer, this information should not necessarily be interpreted as such. Due to the relatively low temperature at which weight loss occurs, and the tendency of these polymers to retain water, it is more probable that the first decomposition region is due to solvent impurities, whereas the second region corresponds to the actual polymer (Figure 2.4).

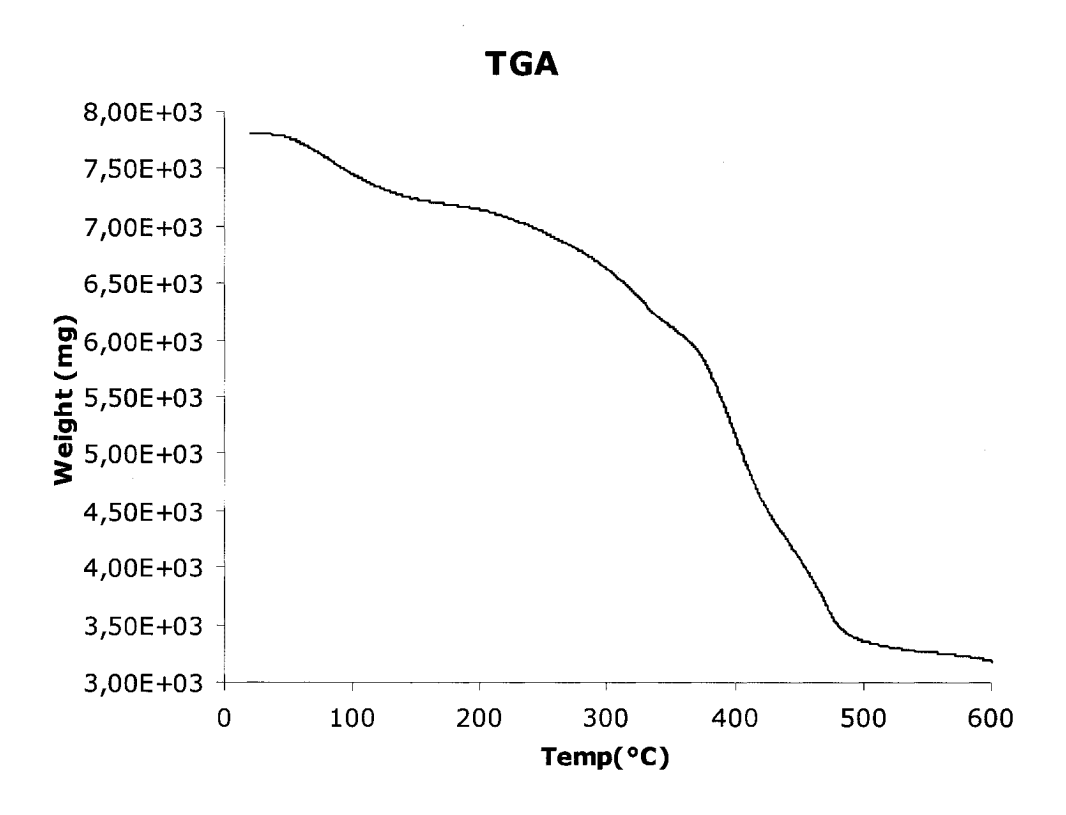
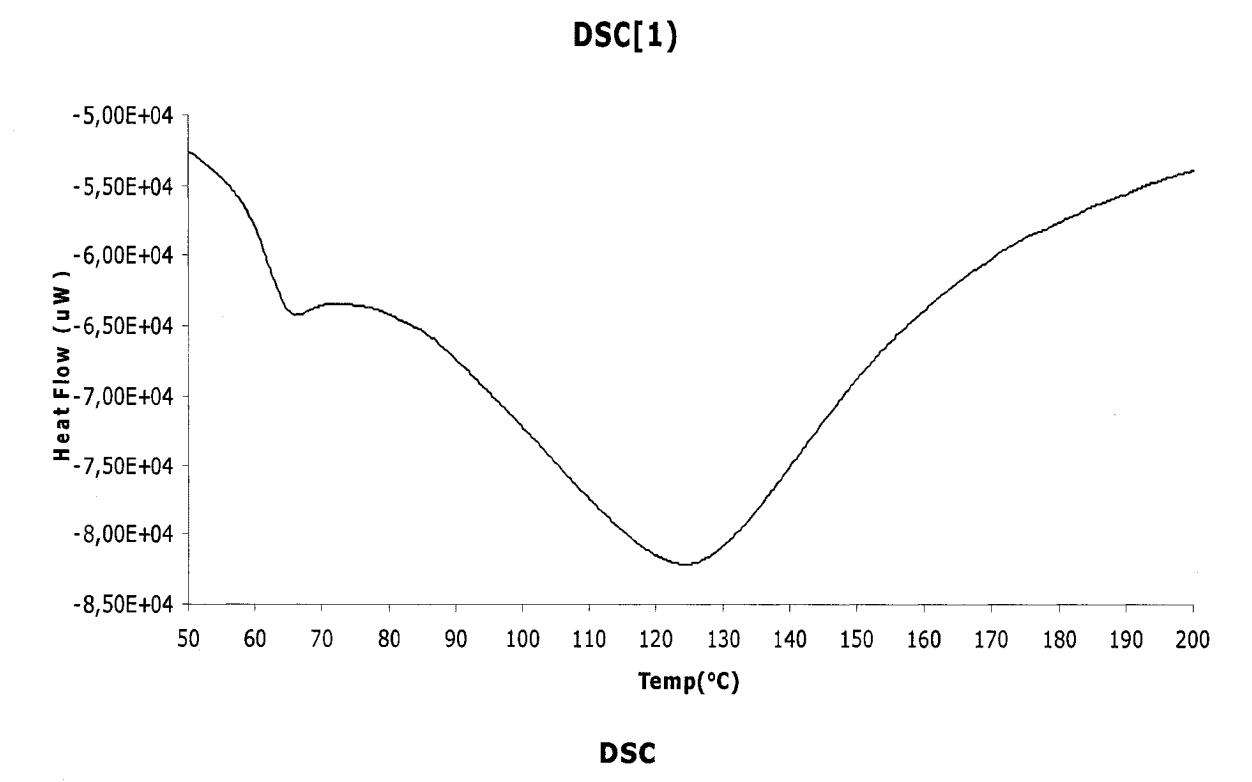


Figure 2.4 Thermogravimetric (TGA) analysis shows decomposition beginning to occur at approximately 150°C. An earlier decomposition is most likely either due to impurities or to water retained in the polymer.

2.4.2 Differential Scanning Calorimetry

Differential scanning calorimetry (DSC) can provide valuable thermodynamic information about polymers when they are heated. The DSC measurements were performed on a Seiko 220 DSC. The original DSC data shows two changes, relating to different compositions of the polymer (Figure 2.5). The first transition could be either due to solvent impurities, or due to poly(acrylic) acid, which had not been attached to the dye. The second transition corresponds to the attached dye and polymer. As the temperature increases past the glass transition temperature, more flexibility is afforded to the polymer, and the two different regions have time to blend together to form one continuous mixture. The second DSC run confirms this as it is taken after the polymer blends together, and only one transition is seen at approximately 140°C, which is interpreted as being the glass transition temperature of the polymer.



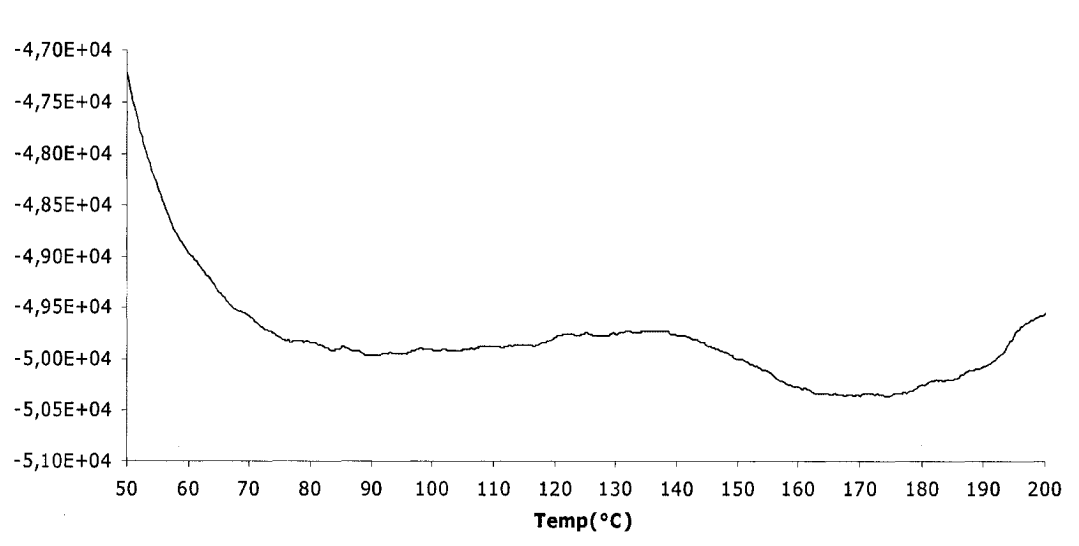
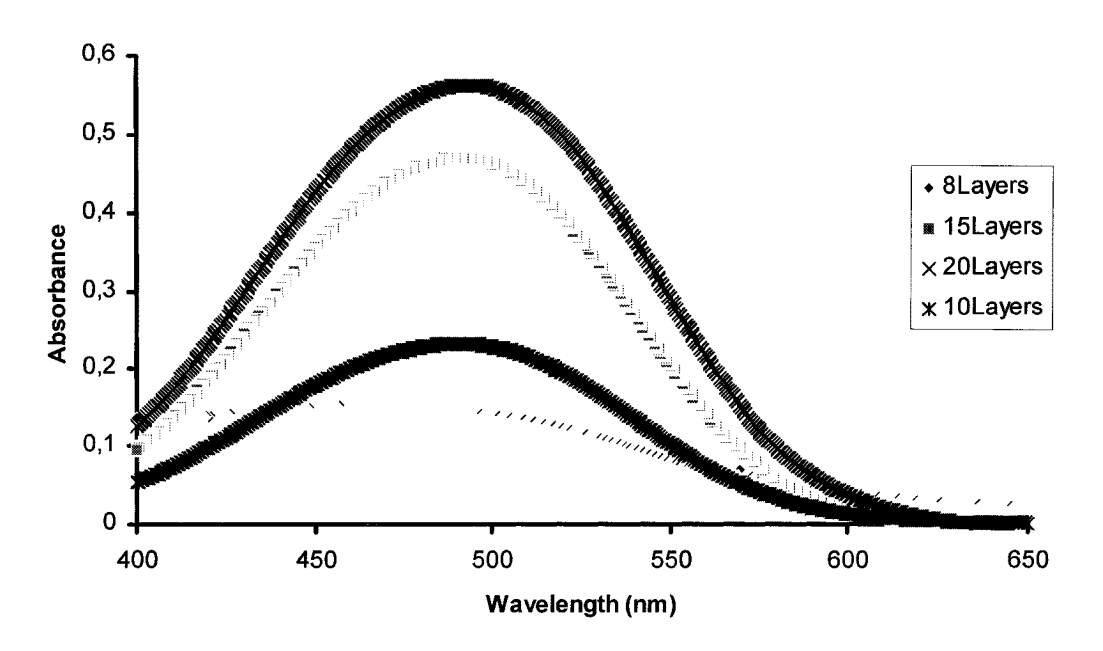


Figure 2.5 Differential Scanning Calorimetry (DSC) results for the first (top) and second (bottom) scans. The first scan shows two clear distinct transitions at approximately 65°C and at 125°. A second scan taken after the polymer was provided enough heat to blend together shows only one transition at approximately 140°C.

2.4.3 Absorption Spectroscopy

Azobenzenes are extremely photoactive, and their absorption ranges in the visible spectra depending on many factors, including solvent, and their degree of functionalization. The three different classes of azos (azobenzenes, stilbenes, and pseudo-stilbenes) all have different absorption bands. To confirm that the polymer was indeed of the pseudo-stilbene class of azobenzenes, and also to determine the wavelength of maximum absorbance, the absorption spectra was taken (Figure 2.6), after deposition on a thin film. The characterization was performed on a Varian Cary 300 Bio UV-Visible Spectrophotometer. The λ -max was shown to be at ~488nm, which corresponded to the pseudo-stilbenes. In solution the λ -max was shown to blue-shift slightly, to 480nm, though the absorbance profile of azos has been shown to change depending on the solvent used. In this case, the interaction with water could account for the slight blue shift. As the amount of azo in the sample increased, by adding more layers, the absorbance was also shown to increase.

Absorbance with Increasing Layer Deposition



PolyDR2 in Water 0,6 0,5 0,4 Absorbance 2.0 0,2 0,1 0 400 450 500 550 600 650 700 750 800 Wavelength (nm)

Figure 2.6 Absorption spectra of the polymer on thin films (top) and in solution (bottom). The absorbance clearly increases with increasing layer deposition. The maximum absorbance shifts from 488 to 474 from thin film to solution.

2.4.4 Ellipsometry

Ellipsometry uses the change in refractive indices of a sample to provide the thickness of the sample. In order for ellipsometry to be successful, the substrate on which the sample resides must be reflective. To ensure that there were no procedural variations while coating the substrates, two different substrates were coated simultaneously in the same solutions, one substrate being a glass slide to measure absorbance, while the second substrate was a clean silicon sample to allow for ellipsometry. The determined value of the thickness for each films was the average of 20 different measurements taking on different spots along the film.

It was essential that each substrate be clean and active. The glass slides were immersed in concentrated nitric acid for 24 hours, rinsed thoroughly with milli-Q water, then heated to activate the surface. The silicon wafers were immersed in a piranha solution consisting of 3:1 H_2SO_4 to H_2O_2 . This solution was gently heated to approximately 90°C and maintained at that temperature for 30 minutes. The substrates were then carefully removed using Teflon tweezers and rinsed thoroughly under Milli-Q water. They were then stored under water until used. Ellipsometry measurements were performed using a Gaertner L116C ellipsometer. The relationship between thickness and absorbance is shown in Figure 2.7. The resulting extinction coefficient, $\varepsilon = 0.8 \mu \text{m}^{-1}$ is approximately 6X less than that of PDR1 ($\varepsilon = 5.30 \mu \text{m}^{-1}$) [8].

Determination of PDR2 Extinction Coefficient

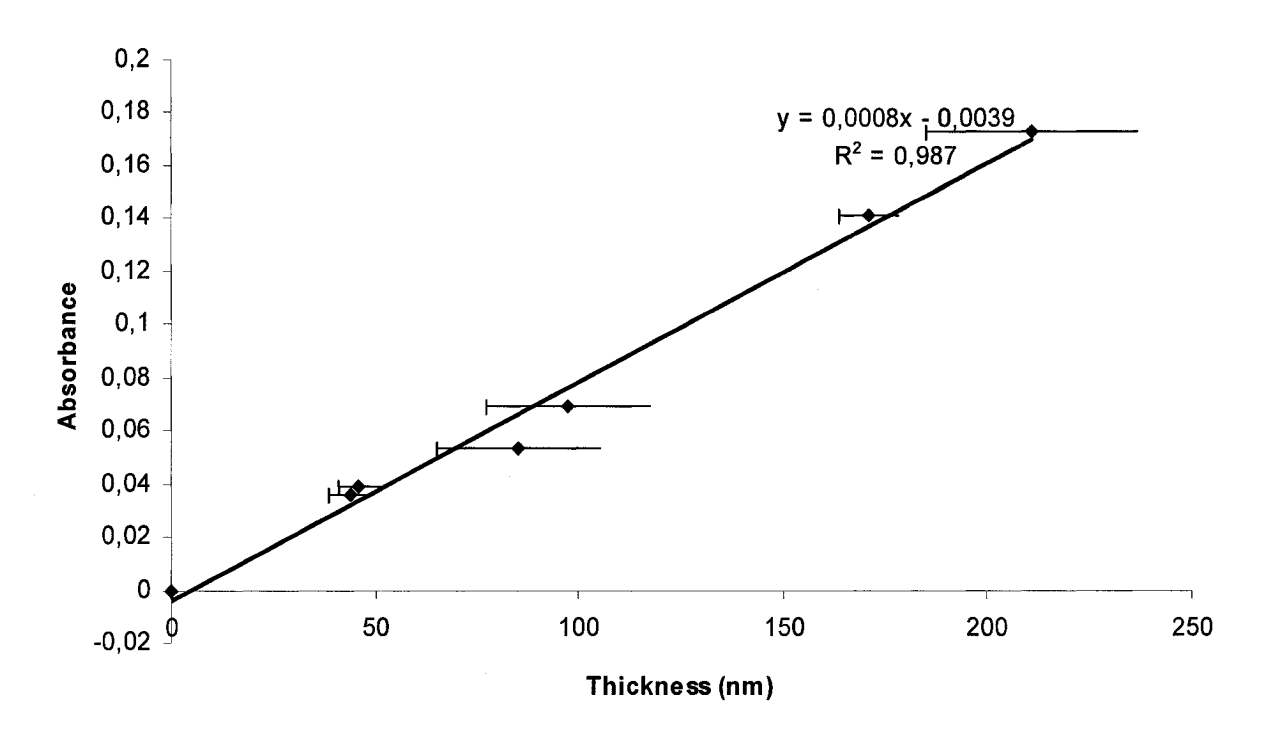


Figure 2.7 Comparing the absorbance of a sample, as determined by UV spectroscopy and thickness, as determined by ellipsometry allows the extinction coefficient, ε , to be determined. It is approximately 5 times less than that of PDR1, which was shown to be $5.30\mu m^{-1}$

2.4.5 Nuclear Magnetic Resonance

Nuclear Magnetic Resonance (NMR) was performed on the polymer with a Varian XL-300 spectrometer to determine whether or not the dye was attached to the polymer, rather than doped in the poly(acrylic) acid backbone, and to confirm the structure of the compound. A broadening of the peaks was interpreted as the azo dye being attached to the polymer. NMR was also used to confirm the absence of side products or other forms of contamination in the polymer before they were coated on the slides through LBLSA.

The structure of the polymer, along with the spectra is shown (Figure 2.8). Going from upfield to downfield in the spectra, the peak furthest upfield at $\delta = 8.3$ is to the 'a' protons on the aromatic portion of the dye, closest to the nitro group. Two peaks are seen intertwined between $\delta = 7$ and $\delta = 8$. The further upfield peak at 7.6 is for the equivalent 'b' protons on either side of the azo bond, on the aromatic portion of the dye, whereas the peak at 7.2 is due to the 'd' proton attached to the nitrogen in the amide bond. At $\delta = 6.8$, a peak resulting from the final aromatic protons, 'c', is shown. Further downfield at $\delta = 3.7$, a peak is seen due to the 'e' protons which are adjacent to the amide bond. Between $\delta = 0$ and $\delta = 3.0$, multiple peaks are seen which correspond to the poly(acrylic) acid backbone. The spectrum looks free of contamination, and there appears to be no trace of leftover starting material either.

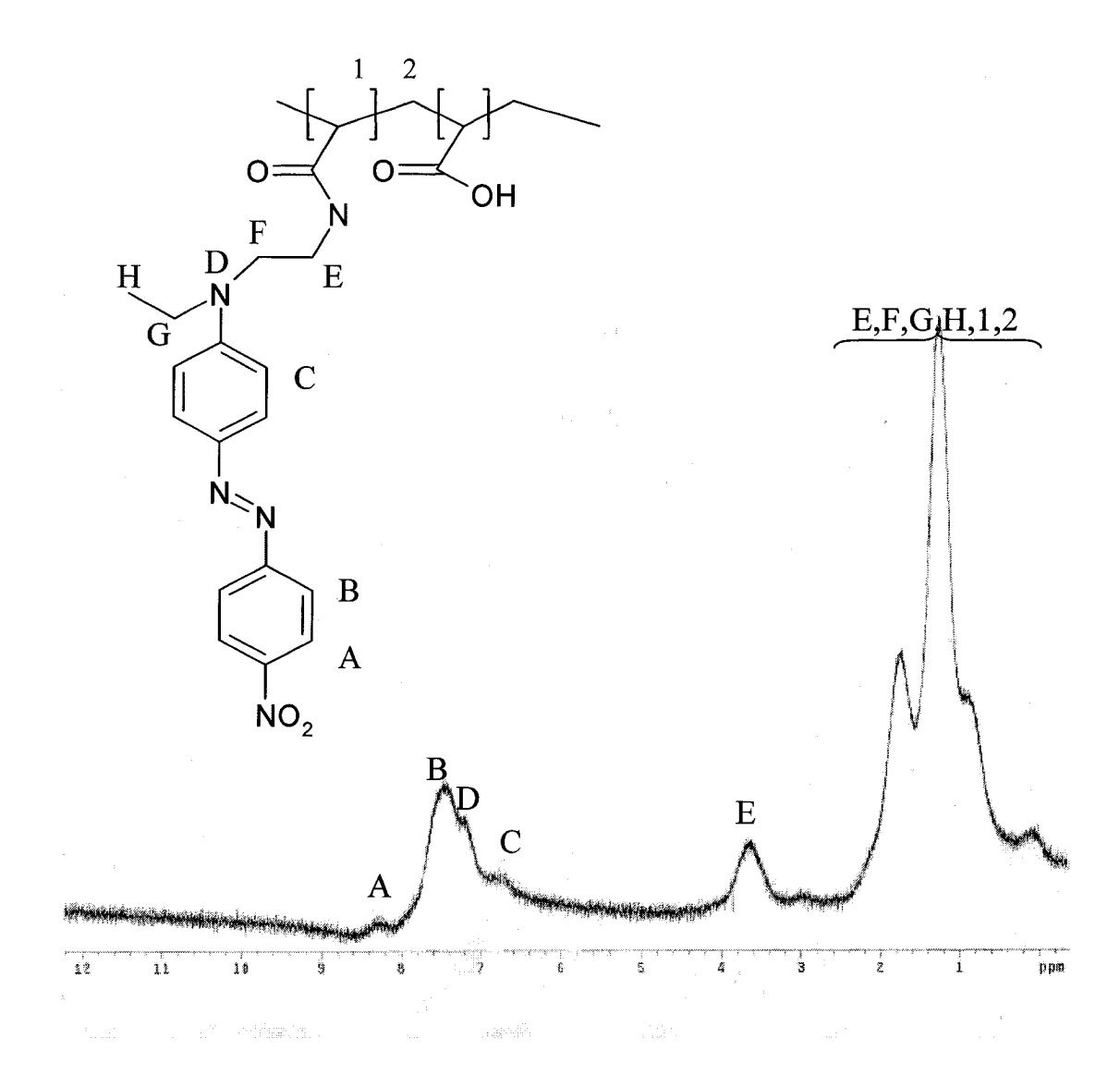


Figure 2.8 An NMR of PDR2 with the peaks labeled. A lack of unlabeled peaks indicates a pure sample.

2.4.6 Gel Permeation Chromatography

Gel Permeation Chromatography (GPC) was performed on the polymer in THF, with a concentration of 4g/L, using a Waters 1515 Isocratic Pump, 2487 Dual Absorbance Detector, 2414 Refractive Index Detector and a set of three Waters Styragel High Resolution Columns (HR1, HR3 and HR4) placed in series. The molecular weight, however, was found to be at the limit of detection, and results are inconclusive, but they indicate that the molecular weight is approximately 2000g/mol.

References

- [1] Natansohn, A.; Rochon, P. Chem Rev. 2002, 102, 4139.
- [2] Yager K.G., Barrett, C.J. Journal of Photochemistry and Photobiology A: Chemistry 2006, 182, 251.
- [3] Hagen, R. Bieringer, T. Adv. Mater. 2001, 13, 1805.
- [4] Ramanujam, P.S.; Hvilsted, S.; Ujhelyi, F.; Koppa, P.; Lorincz, E.; Erdei, G.; Szarvas, G. *Synth. Met.* **2001**, *124*, 145.
- [5] Mermut, O.; Barrett, C.J. Analyst (Cambridge, U.K.) 2001, 126, 1861.
- [6] Barley, S.H.; Gilbert, A.; Mitchell, G.R. J. Mater. Chem. 1991, 1, 481.
- [7] Jiang, Y.; Han, H.; Chengzhi, Y.; Vass, So.O.; Searle, P.F.; Browne, P.; Knox,R.J.; Longqin, H. J. Med. Chem. 2006, 49, 4333.
- [8] Yager, K.G.; Tanchak, O.M.; Godbout C.; Fritzsche, H.; Barrett, C.J. *Macromolecules* **2006**, *39*, 9311.

Chapter 3

Effect of Humidity on Quantum Yields and Birefringence

3.1 Introduction

Polyelectrolyte multilayers (PEMs) are prepared by sequentially dipping a charged substrate into solutions of oppositely charged polyelectrolytes. They have gained considerable interest in recent years in material applications due to the facility with which their properties can be tuned. Film thickness and surface properties can be controlled in weak polyelectrolyte systems through various factors, including pH and ionic strength. The ease at which the films can be assembled and the ability to introduce functional groups into the multilayers makes PEMs suitable for applications such as sensors [1] and drug delivery vehicles [2]. The ionic character of the internal cross-link points and the free acid/base groups makes their interaction with water complex. It has been shown that PEM pre-exposure to various humidity environments can greatly influence bulk water uptake, where the rate of swelling could be varied by three orders of magnitude, simply by modifying the relative humidity prior to exposure to water [3]. Films pre-exposed to high humidity required a longer time to reach saturation when swollen with bulk water. This was the opposite result of what was expected, which is that pre-exposure to high levels of water vapour would plasticize the multiplayer and accelerate the swelling. The sensitivity of PEMs to

water vapour content may be attributed to structural changes in the film and/or water organization within the film.

It has been found that water distribution within the weak polyelectrolyte thin films is asymmetric. Localization of the water molecules occurs preferentially at the polymer surface [3,4]. This variation with humidity might not be limited to swelling properties, but may also influence intrinsic properties of azo materials. They have already been shown to influence relaxation times, which relate to how rapidly the azo chromophore in *cis* form relaxes to the *trans* form thermally, therefore it is conceivable that other factors related to the photoisomerization, such as quantum yields, may also be affected.

3.2 Quantum Yields

In the system under study, the obvious change upon photon absorption is the familiar *trans* to *cis* isomerization, and this photoisomerization was the basis for which quantum yields were measured. The determination of quantum yields was performed primarily using a method advanced by Dumont [5]. and was a combination of Fischer's method and Rau's method. Fischer [6] had originally devised a method to determine quantum yields through purely spectroscopic data, allowing quantum yields to be determined for compounds with meta-stable *cis* states. Rau [7] modified Fischer's ideas and developed a method to circumvent the problem of thermal

reconversion for the *cis* states. The derivation of all these equations can be found in detail in these papers [5,6,7].

The absorbance of a film with more than one species present is equal to the sum of the concentrations of the species times their respective extinction coefficients. For azobenzene films:

$$A_o = \varepsilon_t[\text{trans}]_o l + \varepsilon_c[\text{cis}]_o l \tag{1}$$

Where l is the total film thickness and ϵ is the extinction of that species at a specific wavelength.

To determine the composition of the photostationary state, the extinction coefficients of the *trans* and *cis* isomers (ϵ_t and ϵ_c) at the pump wavelength must be known. The *trans* species is stable and can be isolated and concentration and absorption measurements can be used to provide ϵ_t . Once the composition of the photostationary state can be estimated, the quantum yields can be determined for the *trans-cis* photoisomerization (Φ_{tc}) and the reverse *cis-trans* (Φ_{ct}) photoisomerization. Photochemical characterization of thermally unstable species, such as the *cis* isomer of azobenzene cannot be carried out directly, and in 1967 Fischer published a method for determination of the composition of the photostationary state, and hence, ϵ_c . This method was later generalized by Rau to account for systems in which the *cis* state thermally reconverted to the *trans* state. Finally, Dumont combined these ideas and applied them to thin films of azo polymers.

Dumont's method relies on the assumption that the equations governing the photostationary state apply equally well tin thin films as in solution. Dumont used Fischer's method, which allowed ϵ_{cis} to be determined at any wavelength, and Rau's method, which allowed the problem of thermal reconversion to be circumvented. In these experiments, two wavelengths with unlike A values were used to provide three sets of pump/relax curves irradiating and probing either on λ -max (488nm) or on the shoulder of the same band. The three sets of experiments were:

Set 1: Irradiation at 488nm, Analysis at 488nm

Set 2: Irradiation at 514nm, Analysis at 514nm

Set 3: Irradiation at 514nm, Analysis at 488nm

Rau [7] modified Fischer's method to circumvent the problem of thermal reconversion for the *cis* states. He realized that the dominant reconversion process depended on the intensity of irradiation, with thermal relaxation playing a larger role than *cis-trans* photoisomerization at low irradiation intensity. At infinite irradiation, the thermal reconversion would be negligible. With this intensity dependence, a series of pump/relax measurements of Δ could be made over a range of pump intensities to extrapolate to infinite intensity, allowing for the estimation of Δ^{∞} , the difference between A_{0} and A_{∞} at infinite intensity.

During irradiation, [cis] is given by:

$$d[cis]/dt = 1000I'_{o}(1-10^{-A'})(\epsilon'_{t} \Phi'_{trans}[cis] - \epsilon'_{c} \Phi'_{cis}[cis])/A'-k[cis]$$
 (2)

The primed quantities refer to measurement at irradiation wavelength, the unprimed ones refer to the analysis wavelength. I_0 is the incident photon flux, A' is the total absorbance of the sample, and k is the thermal *cis-trans* isomerization rate constant. The factor 1000 is required as a conversion factor when I_0 is expressed in Einsteins per cm², and is obtained by realizing that $1L = 1000 \text{cm}^3$.

If σ is the molar fraction of [cis] in the photostationary state, equation 2 can be rewritten as:

$$d\sigma/dt = F'(t)\epsilon'_t \Phi'_{trans} - (F'(t)Q' + k)\sigma$$
(3)

where

$$F'(t) = 1000I'_{o}(1-10^{-A'})/A'$$
(4)

and

$$Q' = \epsilon'_t \Phi'_{trans} - \epsilon'_c \Phi'_{cis}$$
 (5)

In the photostationary state $d\sigma/dt = 0$, and

$$\varepsilon'_{t} \Phi'_{trans} = (F'_{o}Q' + k)\sigma_{o}/F'_{o}$$
 (6)

The total absorbance from equation (1) can be expressed as a function of σ with:

$$A(t) = \varepsilon_t[\text{trans}] + \varepsilon_c[\text{cis}] = [(\varepsilon_c - \varepsilon_t)\sigma + \varepsilon_t][\text{azo}]$$
 (7)

Combining equations (6) and (7), applying the conditions for the photostationary state, and simplifying, the measured quantity Δ can be expressed as a function of quantum yields, extinction coefficients, total absorbance, and pump beam intensity:

$$\frac{1}{\Delta} = \frac{\epsilon'_{t}\Phi'_{tc} + \epsilon'_{c}\Phi'_{ct}}{(\epsilon_{c} - \epsilon_{t})A'_{t}\Phi'_{tc}} + \frac{k}{1000(\epsilon_{c} - \epsilon_{t})A'_{t}\Phi'_{tc}} X$$
(8)

where

$$X = A'_{0}/(1 - 10^{-A'_{0}})I_{0}$$
 (9)

A plot of Δ^{-1} vs X over a series of irradiation intensities should be linear and allow Φ'_{trans} to be determined from the slope. This value can then be used to determine Φ'_{cis} from the intercept with experimentally determined ϵ_t and ϵ_t , and using Fischer's method to determine ϵ_c and ϵ_c .

Fischer's method was introduced for systems without thermal relaxation and the notation " ∞ " means that the data has been extrapolated to infinite intensity. The extrapolated photostationary state can be estimated by measuring the absorption spectra after a photostationary state has been reached by irradiation at two different wavelengths. The ratio of equilibrium concentrations are given by:

$$[trans]_{0}^{'\infty}/[cis]_{0}^{'\infty} = \epsilon'_{c} \Phi'_{cis}/\epsilon'_{t} \Phi'_{trans} = \Phi'_{cis} A'_{c}/\Phi'_{trans} A'_{t}$$
 (10)

The results of irradiation of any two wavelengths λ' and λ'' with differing extinction coefficients, the ratio of the equation

$$[\text{trans}]_0^{" \infty} / [\text{cis}]_0^{" \infty} = \varepsilon_c^" \Phi_{\text{cis}}^" / \varepsilon_t^" \Phi_{\text{trans}}^" = \Phi_{\text{cis}}^" A_c^" / \Phi_{\text{trans}}^" A_t^"$$
(11)

Leads to $\Phi'_{cis}/\Phi'_{trans}$ and $\Phi''_{cis}/\Phi_{trans}$ canceling out as long as the ratio does not depend on the wavelength of irradiation.

If α^{∞} represents the extent of *trans-cis* conversion at infinite intensity, then:

$$[\text{trans}]_0^{\infty} / [\text{cis}]_0^{\infty} = (1 - \alpha^{\infty}) / \alpha^{\infty}$$
 (12)

Total absorbance can be described as

$$A = A_{\infty}(1 - \alpha^{\infty}) + A_{c}\alpha \tag{13}$$

This is also valid when the infinite flux photostationary state is considered:

$$A_{c} = A_{t} + \Delta \alpha / \alpha \alpha \tag{14}$$

If δ'^{∞} and δ''^{∞} denote the relative change of absorbance at the two wavelengths when the photostationary state is estimated with infinite intensity, then we get:

$$\frac{\left[(1-\alpha^{\infty})/\alpha^{\infty}\right]}{\left[(1-\alpha^{\infty})/\alpha^{\infty}\right]} = \frac{\left[(1+\Delta^{\infty}/A_{t}^{\alpha}\alpha^{\infty})\right]}{\left[(1+\Delta^{\infty}/A_{t}^{\alpha}\alpha^{\infty})\right]} = \frac{\left[(1+\delta^{\infty}/\alpha^{\infty})\right]}{\left[(1+\delta^{\infty}/\alpha^{\infty})\right]}$$
(15)

Fischer's equation (16), which gives $\alpha^{n^{\infty}}$ as a function of parameters which can all be measure experimentally, is then yielded.

$$\alpha^{\prime\prime\prime\alpha} = (\delta^{\prime\prime\alpha} - \delta^{\prime\prime\alpha})/[1 + \delta^{\prime\alpha} - \rho(1 + \delta^{\prime\prime\alpha})]$$
 (16)

The ratio ρ is introduced as $\alpha'^{\circ\circ}/\alpha''^{\circ\circ}$ at the two different excitation wavelengths, and is equal to the ratio of the Δ 's measured at the maximum wavelength when irradiating with wavelength λ' and λ'' . The value of $\alpha''^{\circ\circ}$ from equation (16) can be used to calculate the extinction coefficient of the *cis* isomer using equation (14). Using equation (8), the quantum yields can then be determined. It should be noted that ϵ_t refers to optical density and can be calculated by using α , the amount of chromophore in the *trans* state, and the chromophore density.

To construct the Rau plots, the laser power was altered between 7 - 80 mW per cm². At the lower intensity, this still allowed for the signal to noise to be distinguished clearly, minimizing instrumental error, and at the higher intensities, it allowed us to measure the films without burning them. Also, the higher irradiation intensities allowed for the probe light to be distinguished clearly. At higher intensities, scattered light would still find its way into the detector.

Raw Data for Increasing Intensity of PDR2

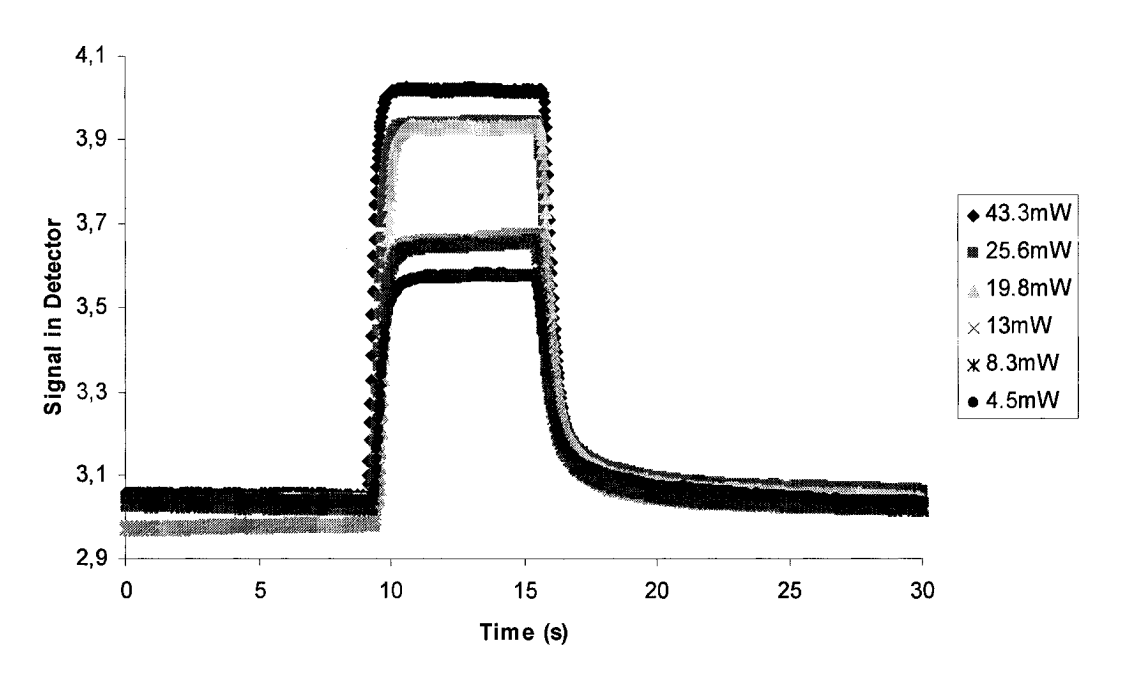


Figure 3.1 Pump-probe experiments for increasing intensity of the pump beam on a 15L PDR2 sample at 43% humidity with both pump and probe at 488nm. Extrapolation of this data allows Δ to be determined.

Great care was taken to ensure that everything about the experiment was kept consistent with only the humidities changing, from experiment to experiment. It was seen that differences arose based on whether or not there was a steady stream of nitrogen running through the chamber, which increased the noise in the probe, and also the rate at which the nitrogen was pumped. It was decided that once the desired humidity was attained, and the samples allowed to equilibrate in that humidity for 24 hours, the chamber would be sealed airtight, and no nitrogen would flow.

The raw data from all the different trials with increasing irradiation intensity is shown in Figure 3.1. The corresponding Rau plot obtained from this data is shown in Figure 3.2.

Rau plot of 15-Layer DR2 at 43% Humidity 5000 10000 15000 20000 25000 30000 35000 40000 45000 50000 -8 -9 514-514 (pump-probe) 488-488 (pump-probe) * 514-488 (pump-probe) -10 1/delta -0,0008x - 7,3108 -11 $R^2 = 0.981$ y = -0.0001x - 7.9327-12 $R^2 = 0.9404$ -0,0007x - 7,1707 $R^2 = 0,9918$ -14 -15 X

Figure 3.2 A Rau plot of a 15L PDR2 sample at 43% humidity. This contains the information for all three sets of data and quantum yields can be ascertained from these plots.

Unfortunately, due to the close strong absorbance of the compound at 514nm, the lines for sets 2 and 3 were very similar. However, this was consistently seen for every set of data, and the overall trend of quantum yields is still justified.

3.3 Birefringence

The azo chromophore can be photo-aligned with polarized light due to a statistical absorption and reorientation phenomenon [8]. Azobenzenes preferentially absorb light that is polarized along the long axis of the molecule. The probability of absorption varies with $\cos^2\theta$, where θ is the angle between the light polarization and the azo dipole axis, meaning that azos oriented along the polarization of the light will absorb, while those whose orientation is against the light polarization will not. At a given angular distribution of chromophores, some will absorb and isomerize to the *cis* state, then revert back to the *trans* form in another new random direction. Those chromophores that fall perpendicular to the light polarization will no longer isomerize and reorient, resulting in a net depletion of chromophores aligned with the light polarization. This reorientation is fast and gives rise to birefringence and dichroism [9]. Circularly polarized light will randomize the chromophore orientations again, making the reorientation process reversible (Figure 3.3). This fully reversible chromophore alignment leads to strong dichroism and birefringence in the azo materials, due to the azos' anisotropic structure.

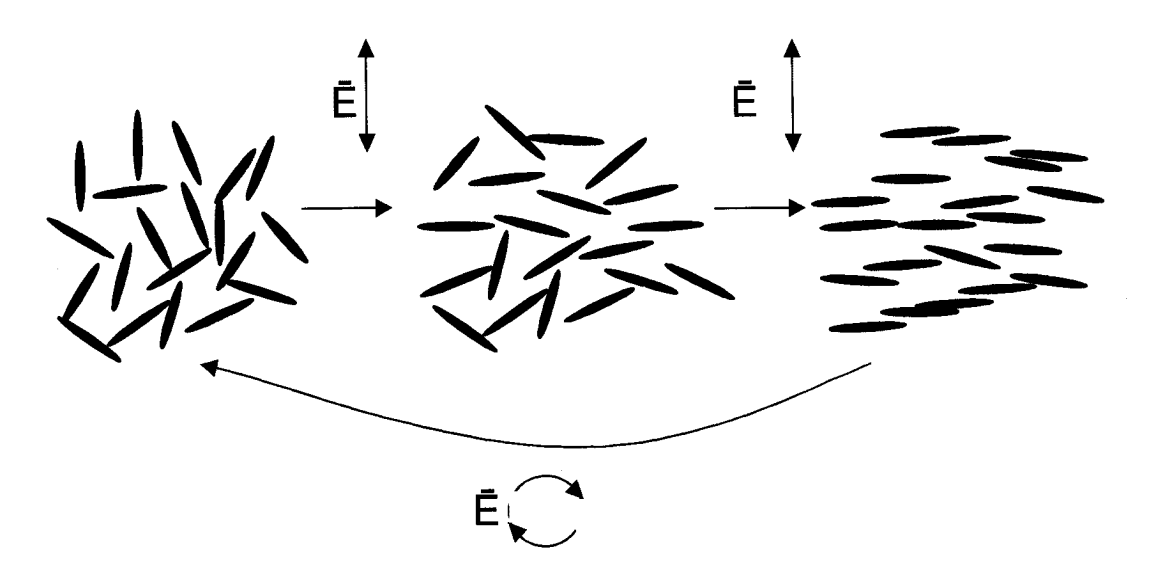


Figure 3.3 Irradiation causes the azo chromophores to absorb the light, isomerize, and randomly reorient while relaxing. Those azos perpendicular to the light cannot absorb and the end result is alignment perpendicular to the incoming light. This is known as statistical reorientation. Random orientation can be restored by irradiating with circularly polarized light.

The mechanism by which birefringence is obtained is based on photoinduced *trans-cis-trans* isomerization of the azobenzene groups, accompanied by their movement and re-arrangement perpendicular to the laser polarization direction. Several structural factors have been found to influence the orientation process including the polarity of the azobenzene groups [10], their bulkiness [11,12], the structure of the spacer between the azo group and main chain [13]. One other factor that has been investigated is the concentration of the azo chromophore in the polymer film [14]. Birefringence levels increase with increasing azo concentration in a copolymer, though some deviation has been noticed.

3.4 Optical Setup – Quantum Yields

The optical configuration used to measure the Quantum Yields can be seen in figure 3.4. The pump beam has been adjusted to 488nm on one laser, and 514nm on the other. The pump beam originates from the laser, and is redirected through a mirror into a splitter, where approximately 5% of the beam is split off. This 5% is used as the probe beam. For the pump, the remaining 95% is then directed, using a mirror, at the sample. Before irradiating the sample, the pump passes through neutral density filters, which are adjusted to vary the power of the pump beams, and through a quarter wave plate, adjusted to ensure that the laser beam is circularly polarized.

The probe beam, which was the remaining 5% split off of the pump beam is also re-directed back at the sample, though it is important to ensure that the probe beam hits the sample directly, and not at an angle. Before hitting the sample, the probe beam must pass through neutral density filters, a converging lens, and a chopper, in that order. The neutral density filters are used to ensure that the probe beam is at a sufficiently low intensity so as not to cause any sort of isomerization in the azo sample.

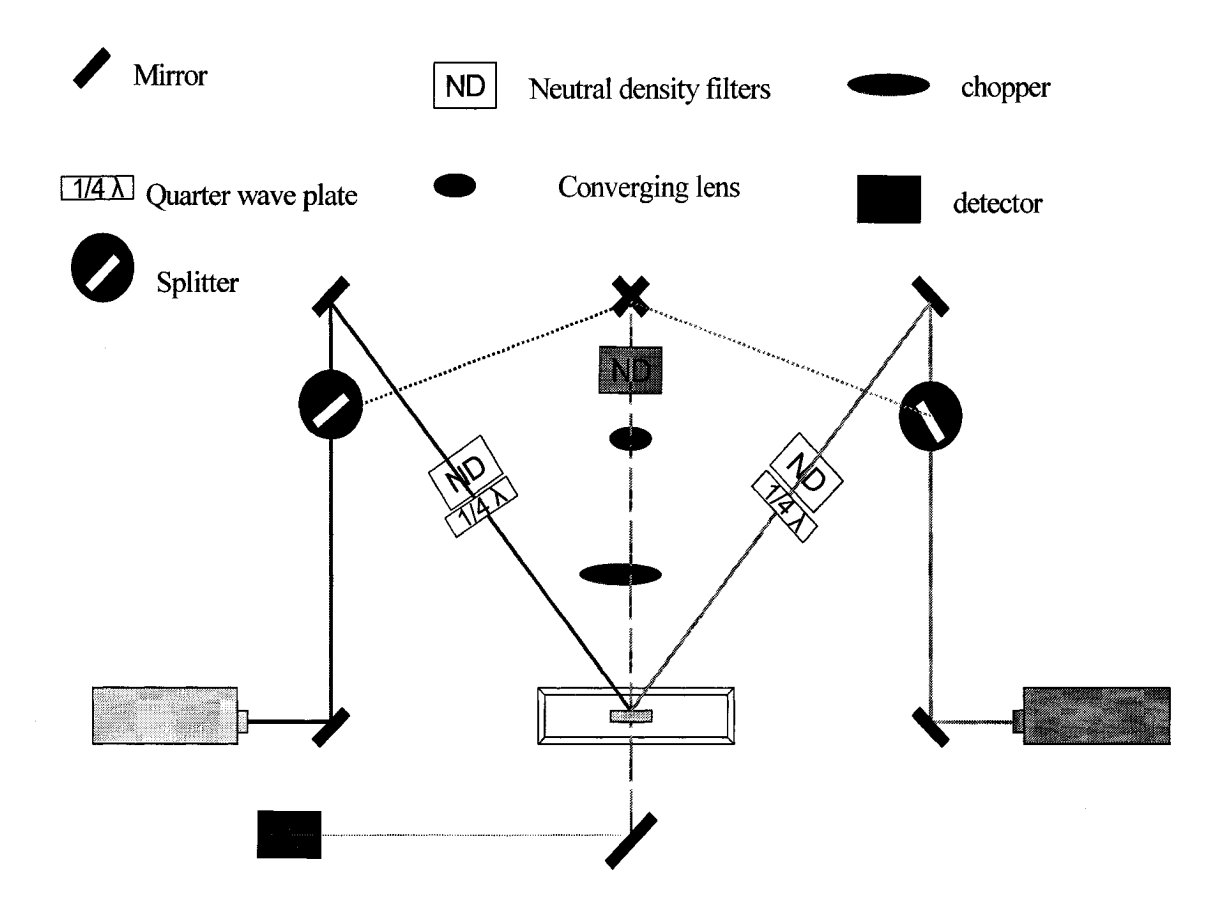


Figure 3.4 A schematic of the quantum yield experiment. Two air-cooled Ar⁺ lasers identifying the 488nm (blue) and 514nm (green) wavelengths. Each laser can act as either the probe or the pump depending upon the specific experiment. The pump lines are identified as solid lines, the probe lines are dashed. After passing through the sample, the probe beam is bounced off a mirror and into the detector. The beams can be turned on of off via a shutter.

Due to the sensitivity of the azo thin films, the probe beam can be anywhere between 3 and 4 orders of magnitude less than the pump. The converging lens allows for a specific, pinpoint area of the sample to be probed, which allows for detector opening to be smaller, which reduces the amount of stray light, or artifacts, entering the detector. The chopper enables the detector to accurately detect only the specific

wavelength of light desired by chopping the beam at a certain frequency. After passing through the sample, the probe beam is directed into the detector using another mirror. Great care must be taken to ensure that the stray light of the pump beam is also not directed into the detector, as its intensity is many times that of the probe, and can mask the signal change caused by the isomerization. An identical setup was used for the light of 514nm wavelength. A tunable mirror allowed rapid, and accurate switching between the green and blue probes.

3.4.1 Optical Configuration for Birefringence Measurements

Poly(DR2) was prepared as previously reported and deposited on glass slides through layer-by-layer assembly. The same films as used in quantum yield experiments were the ones used for birefringence. The laser setup to measure birefringence is shown in Figure 3.5. A laser of wavelength 688nm was used as the probe. This wavelength ensured that the probe beam isomerized the azo chromophore minimally. The probe passed through a chopper and into a 45° filter, which only allowed light of a certain polarization to pass through and into the sample. Some of the light was absorbed by the sample, but the remaining entered another 45° filter to cancel out the probe light that had not been absorbed, before finally hitting the detector. Pinholes were used to block stray pump beam from entering the detector.

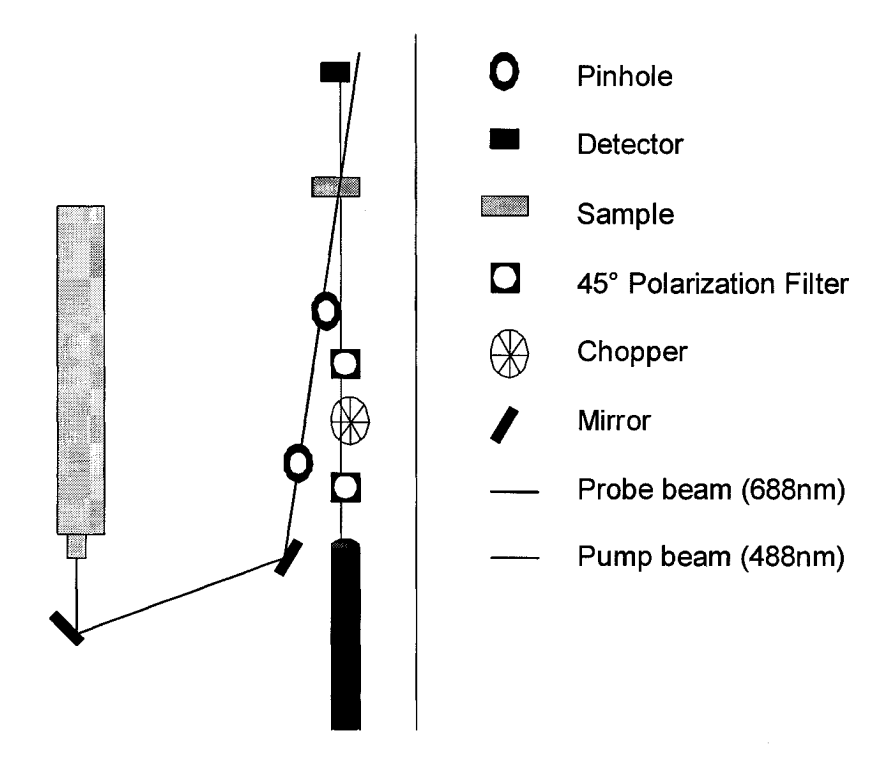


Figure 3.5 The optical setup used for birefringence. The pump beam was tuned to 488nm, the maximum absorbance for PDR2. The chromophores do not strongly absorb the probe beam (688nm) making the analysis undisruptive.

The pump beam was set at 488nm, the maximum absorbance of azo chromophores. It was linearly polarized exiting the laser and was directed to the sample using mirrors. The irradiation caused the azos to isomerize and relax in a direction perpendicular to the incoming polarization.

3.5 Experimental Procedure

The polymer material, poly(disperse red 2) was synthesized as reported in the previous chapter. Samples were prepared by layer-by-layer self-assembly. First the

glass slides were cleaned using a piranha solution consisting of H₂SO₄ and H₂O₂ in a 3:1 ratio. The solution was heated to 90 degrees for 30 minutes, then cooled. The substrates were removed using Teflon tweezers, and rinsed for 5 minutes with distilled water. They were then stored in a water bath until required. The standard procedure involved dipping in a PAH solution for 15 minutes, followed by three rinse baths filled with Milli-Q water for 5 minutes each, followed by immersing in the polymer bath, and again followed by three 5 minute rinse baths. This was followed for each layer, and repeated for as many layers as desired. The films were then left to air dry.

To create an environment of constant humidity, a humidity chamber was designed based on research from Nakamura [15]. The theory behind the humidity chamber involves saturating a solution with different salts and passing nitrogen gas through the cell at a constant flow rate. Adjusting the flow rate was also found to slightly change the humidity. After flowing through the humidity chamber, the gas was flowed through a humidity cell, which was specially designed to allow for quantum yield experiments.

3.6 Results and Discussion – Quantum Yields

Water has been shown to be a good lubricant in PEMs and it might be expected that higher water vapour content in the film would plasticize the film more and allow for more unhindered mobility. Based solely on this reasoning, it would be

expected that as humidity increased, so would quantum yields. However, this was not seen. Instead, it was observed that quantum yields did rise with humidity, to an extent. The quantum yields reached a maximum value at approximately 30% relative humidity (Figure 3.6).

Variation of Quantum Yield with Humidity for 15 Layer Sample

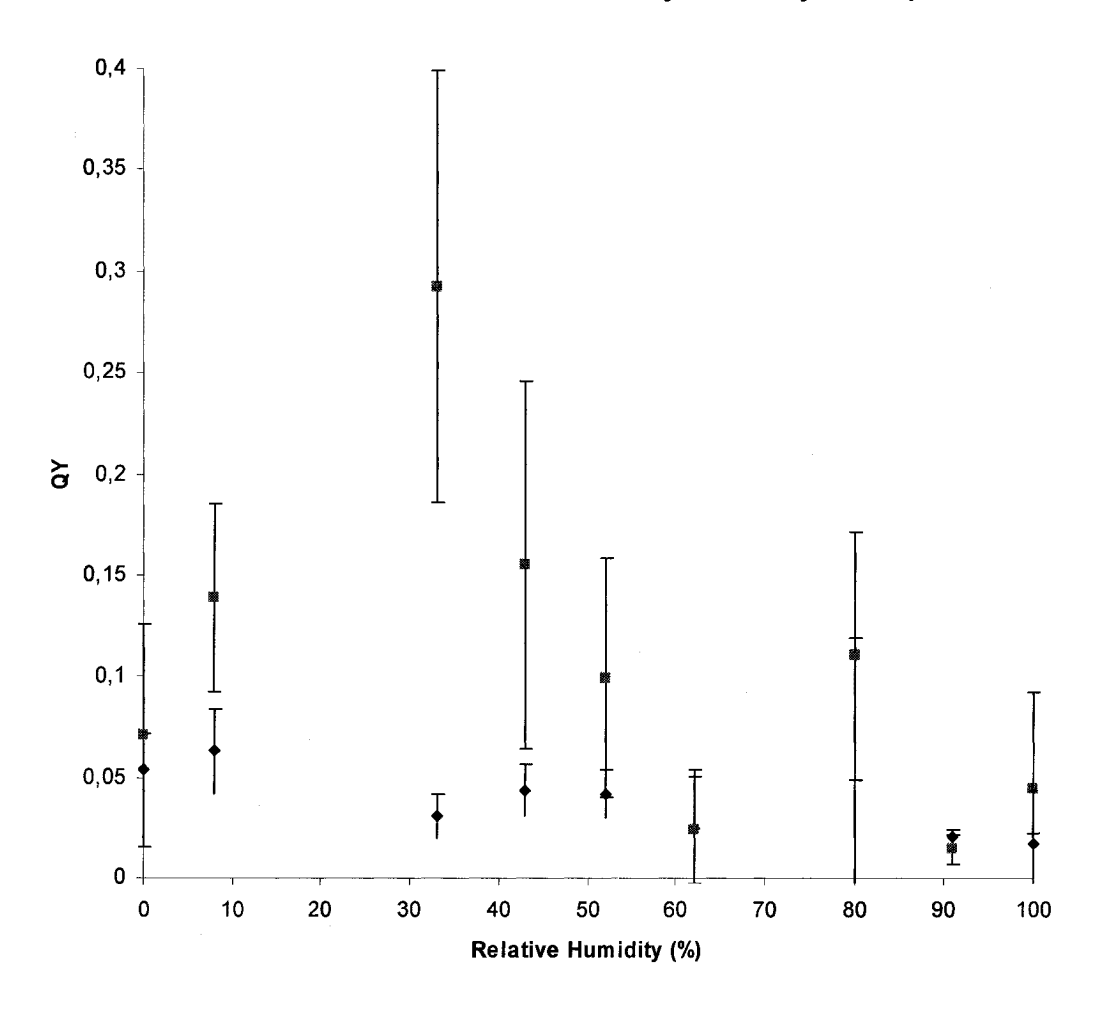


Figure 3.6 A maximum quantum yield can be attained at ~30% relative humidity. Increasing water plasticizes the sample, allowing for easier movement in the polyelectrolyte multilayers, up to a point. Eventually the water molecules can form clusters, resulting in a lower quantum yield.

The errors in the cis to trans quantum yields are much higher than their trans to cis counterparts because the value of Φ_{tc} is required to calculate Φ_{ct} , which compounds the errors. High error rates are common in quantum yield calculations for azo compounds. After reaching a maximum, the quantum yields began to decrease with increased humidity. It is fairly obvious then, that there are more factors involved then the lubrication argument.

To understand what kind of influence humidity and water had on these azo thin films, it is important to understand their dynamics, and to determine which factors can influence quantum yields. The basis of determining quantum yields relies heavily upon the spectroscopic data, which is measured by determining the amount of azo isomerized, which is noticed by an increase in signal due to the less absorbing cis isomer. By measuring the change in signal for various intensities, Δ_{∞} could be determined. The various Δ_{∞} were plotted against humidity (Figure 3.7) to see what role, if any, humidity had upon isomerization.

Change in delta max with Humidity (average 3 sets)

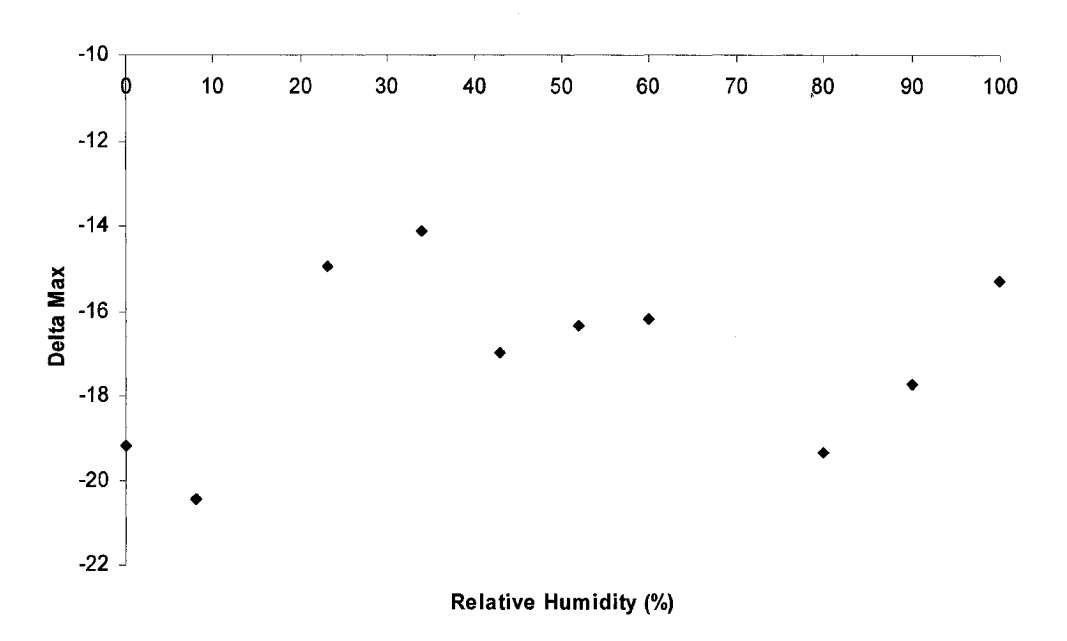


Figure 3.7- Variation of Δ -max with humidity. The Δ -max increases with humidity until a critical humidity after which it begins to decrease, then increase again at very high humidities. These values represent the average of Δ -max of the three sets of data per Rau plot.

Interestingly, the Δ_{∞} values were shown to increase with humidity up to a certain value, which corresponded with the maximum quantum yield, then decreased, and then was shown to increase again. These values corresponded to the ability of the azos to isomerize, which indicated more than a simplistic connection between humidity and the PEM's.

Water, as stated earlier, can act as lubricant in PEM's, however, the interactions between water and PEMs are much more complicated. Experiments on poly azo films based on humidity and water penetration have shown that when a thin polymer film is brought into contact with a penetrating liquid, the penetrant diffuses

into the polymer matrix and the polymer swells [3]. The solvent enters the polymer through pre-existing voids of through spaces that are formed by local segmental motion in the polymer network, which is followed by local relaxation of polymer segments. It is known that water clusters can form around the free carboxylic groups of PAA and that the amount of water clusters associated with PAA is dependent on the humidity [16]. It may be possible for these water clusters to form around counterions within the multilayer. Interactions involving hydrogen bonding with the entangled polymeric loops could results in hydrogen bonded water clusters, which could block the microchannels in the film.

It is conceivable that a similar argument might apply here, as the results indicate that water promotes unhindered motion, up to a certain extent. At low humidity, the polymer network is free of bound water, and as a result, the photoisomerization is unhindered, though the films are not well lubricated. As humidity increases, the films become more plasticized. At high humidity, the highly organized water within the polymer network could slow dynamics.

This does not fully explain what is seen with the isomerizations, as there is an increase in Δ_{∞} values at very high humidities. This can be explained by looking at the swelling dynamics. The swelling dynamics are a good indication as to how much water has penetrated into the layer is the swelling of the polymer film and it has been shown that at very high humidity the swelling actually decreases. This means that less water penetrates into the film and the motion for isomerization is less hindered.

Photoisomerization from *trans* to *cis* also requires a certain free volume, which has been approximated at 0.38nm^3 [17] if isomerization occurs via the rotation pathway, and the penetration of large amounts of water could hinder isomerization. These arguments, though simplistic, may seem valid if the trends of Δ_{∞} values and quantum yields, with respect to humidity, coincided perfectly. However, whereas Δ_{∞} values increase above 90% relative humidity, quantum yields continue to decrease.

Pump-Probe Curve at 62 % Humidity

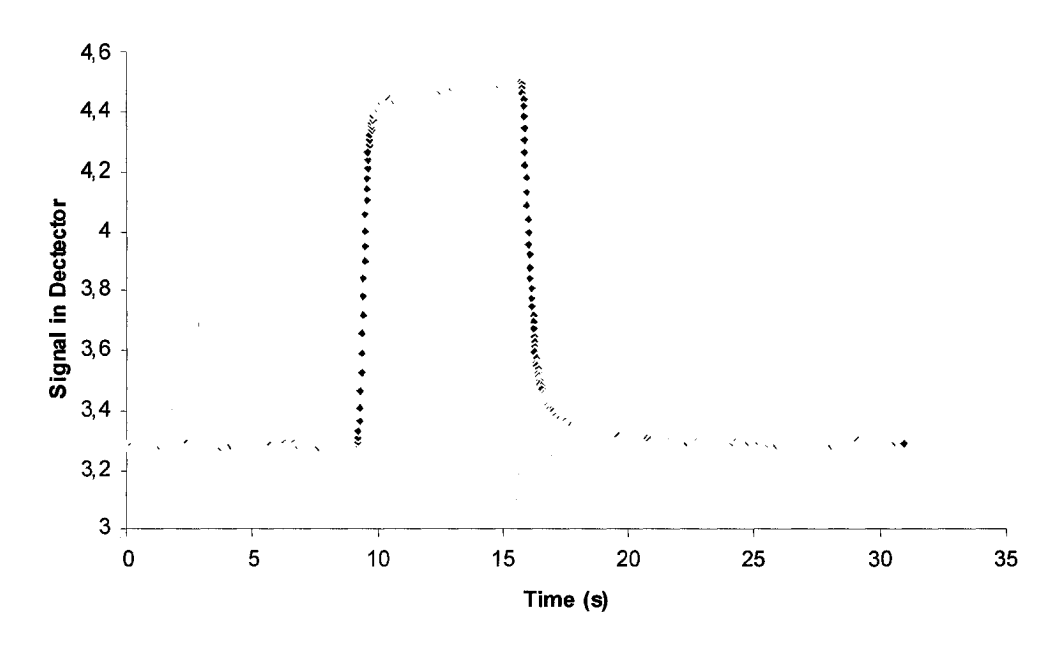


Figure 3.8: A typical pump-probe curve for PDR2. After a baseline is established, the sample is pumped at 9 seconds, at which a rise in the signal is seen due to the isomerization. Irradiation lasts for 6 seconds, after which the signal is reduced back to baseline, due to the relaxation of the *cis* isomer.

Another factor that greatly influences the quantum yields is relaxation rate (Figure 3.9), which is the rate at which the *cis* isomer thermally relaxes to the *trans*

isomer. Higher relaxation rates contribute to a higher $trans \rightarrow cis$ quantum yield, which in turn influences the $cis \rightarrow trans$ quantum yield.

Relaxation Curve of a Pump-Probe Experiment at 62% Humidity

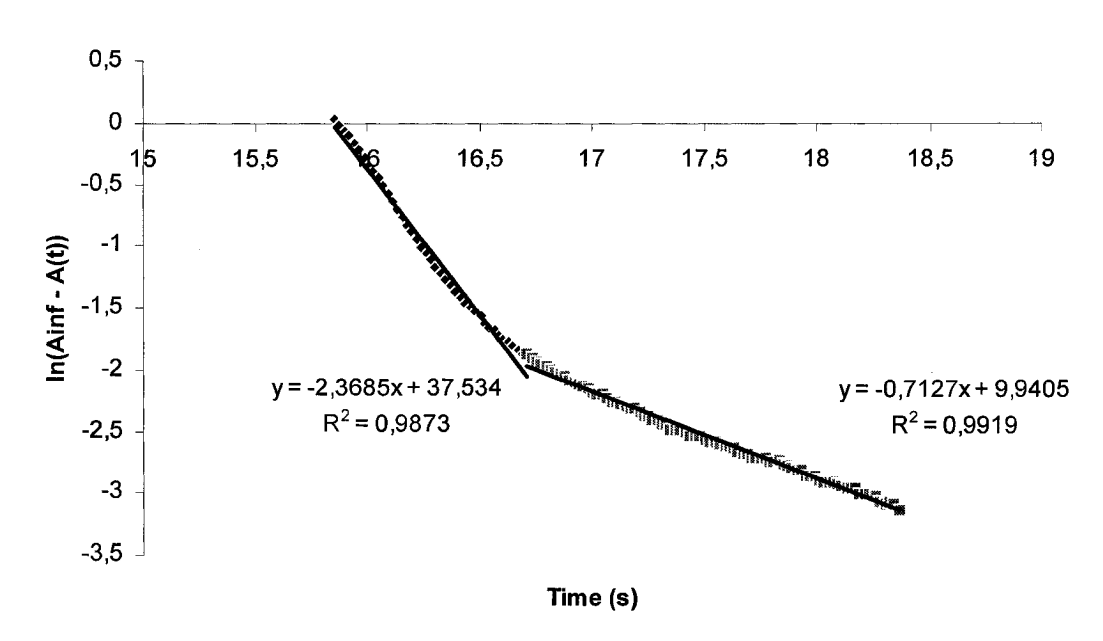


Figure 3.9 A log ($A\infty$ - A(t)) versus time plot of the relaxation clearly shows two distinct regions, a fast relaxation, followed by a slower relaxation. For the purposes of these experiments, only the slow relaxation was use. The fast decay rate has been attributed to *cis* relaxation in strained conformations, or to the translational relaxation of local polymer segments.

Figure 3.10 is a graph that shows the relationship between relaxation rates and humidity. It is apparent that as the humidity increases, the relaxation rate decreases. This has also been seen in other poly azo compounds where relaxation times were found to change by almost an order of magnitude between low and high relative

humidity situations [3,4]. Though the observations here are not that drastic, there is a difference of over 50% between faster and slower relaxation rates.

Influence of Humidity on Relaxation Times

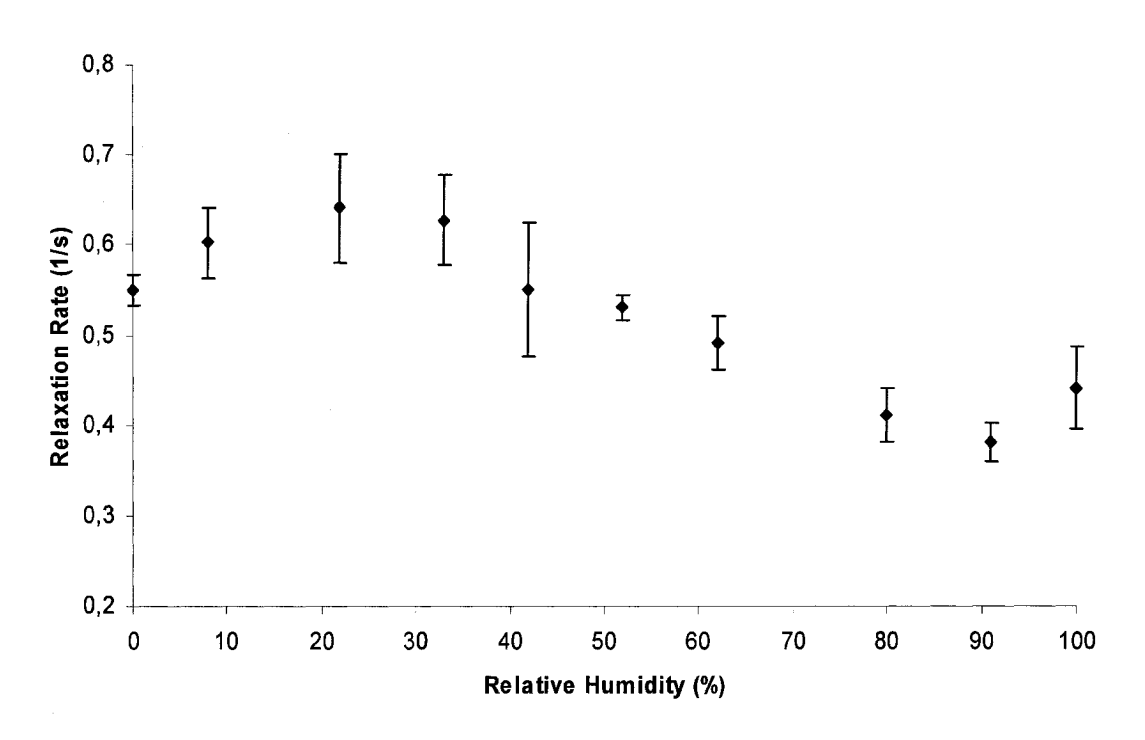


Figure 3.10 Relaxation rates are shown to decrease with increased humidity. This has been suggested to be due to the interaction with the more polar *cis* isomer with water, which delays relaxation.

It is important to note that decay curves for the isomerization tend to show two distinct regions, a fast one and a much slower one. The relaxation rates used for all calculations in this thesis were based on the slower decay. The appearance of the fast decay rate has been studied experimentally on azobenzenes dissolved in the glass state with varying theories as to its cause. Eisanbach [18] attributed it to the occurrence of a translational relaxation of local polymer segments, whereas the slower decay is attributed to rotational relaxation of the neighbouring polymer segments. Other theories [19] suggest that the fast rate is due to relaxation of the *cis* isomer in a strained conformation. It is still unclear what causes the two rates, but modeling experiments [20] suggest that only 14% of the azobenzenes relax anomously fast, so using only the slower relaxation rates is justified.

Ignoring any other effects, it would be expected that as humidity increased, quantum yields would decrease, simply by measuring relaxation rates. However, a similar argument as made for Δ_{∞} values cannot be made to explain the relationship between relaxation times and humidity. The former referred to the $trans \rightarrow cis$ photoisomerization, whereas relaxation rates are a feature of the $cis \rightarrow trans$ thermal relaxation. The decay rate depends on the spectral class of the chromophores and the local environment, so one possible explanation to this trend is the difference in polarity seen between the two isomeric forms of azobenzene, with the cis isomer having a polarity of 3.0 Debye units greater than the non-polar trans isomer [21]. The more polar cis isomer would have stronger interactions with water, which have permeated into the film, reducing the relaxation rate. When there is less water, the interaction is not nearly as strong, or non-existent in some cases, and relaxation rates are greater.

A combination of the two effects, Δ_{∞} values and relaxation rates, offers a reasonable explanation for the relationship between humidity and quantum yields. At low humidities, isomerization is not optimized as not enough water is available to plasticize the films and allow the multilayers to move. As the films become increasingly hydrated, the films plasticize and isomerization occurs. As long as the water content in the film is low enough so as not to interact strongly with the *cis* isomer, relaxation rates are higher. At a critical humidity, shown to be between 30 and 50% in these experiments, the combination of plasticization and higher relaxation rates account for the higher quantum yields. As the films get increasingly hydrated, relaxation rates decrease through interaction with the penetrating water molecules and *trans* to *cis* photoisomerization is hindered through water clusters, resulting in a decrease in quantum yield. At very high humidities the decreased relaxation rates play a more prominent role, and quantum yields are decreased.

3.6.1 Discussion and Results - Birefringence

A typical curve of a polymer with stable birefringence is shown in Figure 3.11. There are three distinct regions of a birefringence curve, a rapid increase in signal as birefringence is induced, a slight decrease due to slight birefringence relaxation, and a rapid drop in signal as circularly polarized light is used to irradiate the sample, essentially erasing the birefringence.

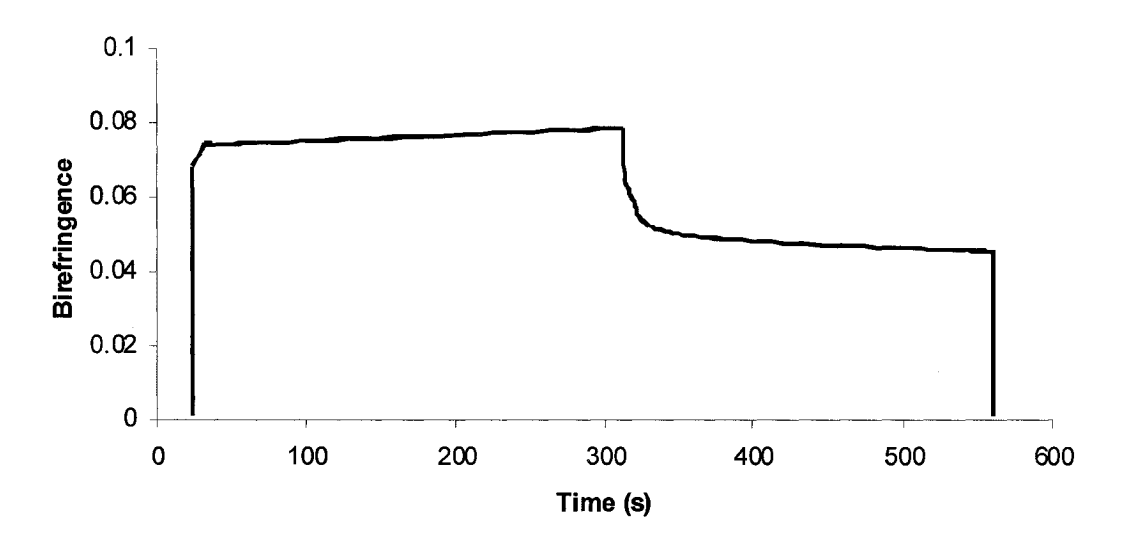


Figure 3.11 A typical birefringence graph shows three distinct regions: a) Rapid signal increase through chromophore alignment b) Slight decrease through relaxation c) Rapid signal decrease upon circularly polarized light.

The rapid increase is due to the alignment of the molecules with the incoming light. As stated earlier, those molecules that are in-line with the irradiation will not absorb, allowing more signal to enter the detector. The slight decrease is due to birefringence decaying to a stable level, and the final drop-off is reverting the molecules back to random orientation. Both the birefringence rise and relaxation can be described using a biexponential and involve "fast" and "slow" contributions. One relaxation process is due to the thermal *cis-trans* isomerization of the azobenzene groups that happen to be in the *cis* state when the writing laser beam is turned off. This phenomenon is specific to azo groups and randomly orients these groups. A second factor is the dipolar interactions between the polar side groups. The local electric field existing in

the film makes it difficult to move polar groups from their equilibrium position, which enhances the stability of photoinduced birefringence.

The typical birefringence curve was not observed with the PDR2 samples tested (Figure 3.12). Although the samples did exhibit birefringence, they did not retain a stable birefringence state. The rise upon irradiation is clearly seen, but as other azo samples retained a stable state, the PDR2 samples relaxed back to a randomly oriented configuration. Figure 3.13 shows the fitting for the biexponential rise and decay.

Birefringence of PDR2 at 60% humidity

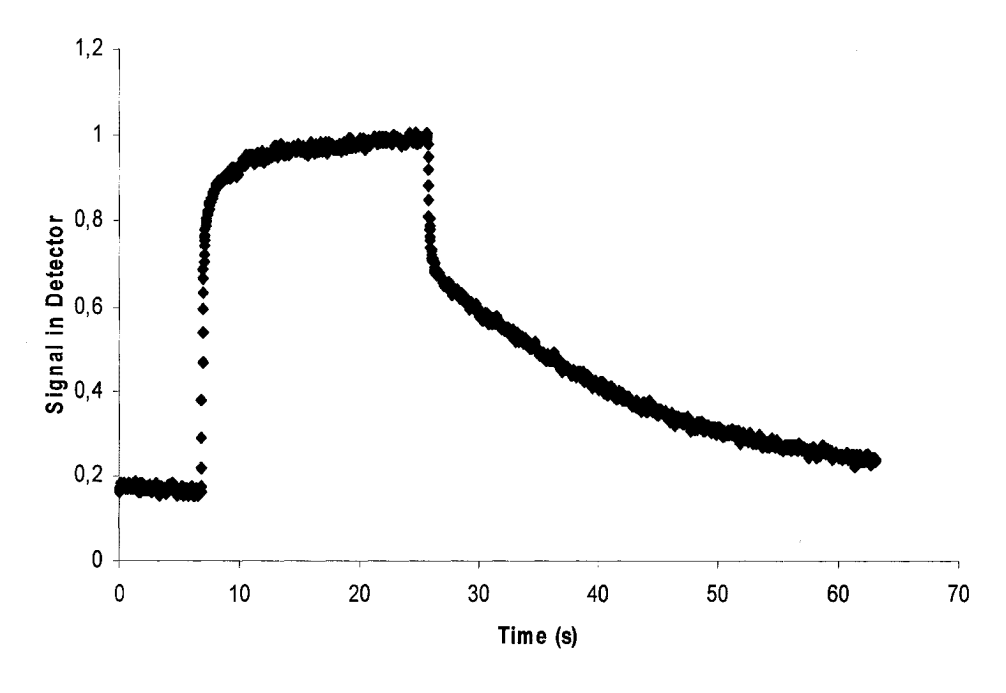


Figure 3.12 The birefringence curve of PDR2 at 60% relative humidity. An increase in signal is seen, corresponding to the alignment of the chromophore, but the chromophores relax rapidly on their own to a random alignment.

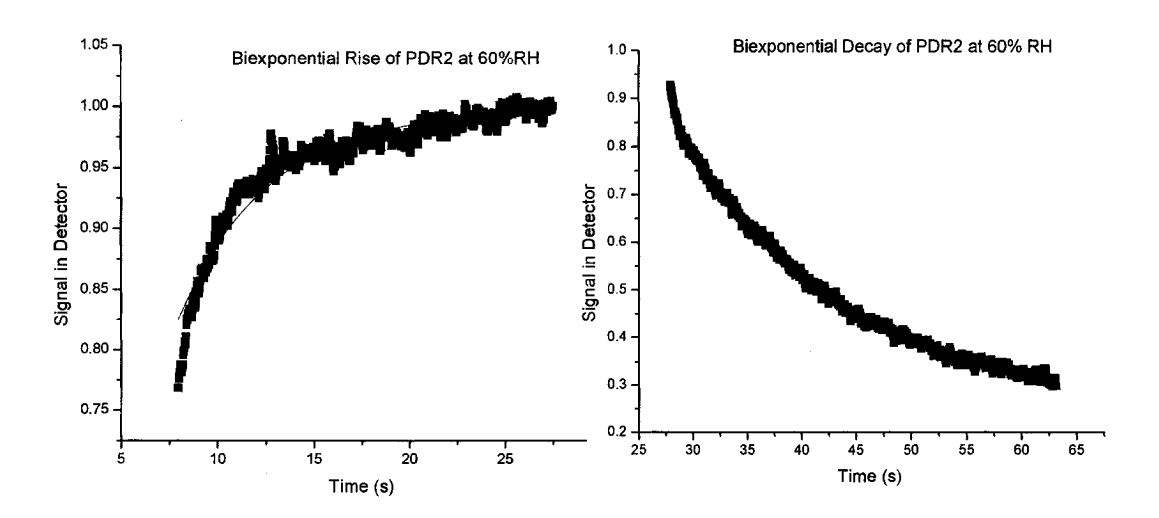


Figure 3.13 The biexponential rise and decay of PDR2 and 60% humidity caused by birefringence.

There could be many reasons why stable birefringence was not observed. The primary reason is due to the low concentration of azo in the films. The azo content was less than 1% for most samples tested, though higher azo content, 4% of DR2, were also tested, and again, it was shown that there was no stable birefringence state. As stated earlier, the dipole interactions between polar side groups are a factor. A sample where the polarity of the side group is similar to that of the azo would allow for more stability. In this case, due to the low azo content, as the azo orients itself, its neighbouring molecules are the poly(acrylic acid) backbone, which may not interact with the azos strongly enough to retain a stable birefringence state. A steric factor has also been proposed as affecting birefringence, in that the size of the comonomer groups plays a role in the reorientation process. A smaller group allows the azo

groups to have a higher degree of freedom, making it easier to randomize when a small side group is present. This has been shown in other samples involving NBEM and the much smaller styrene group (Figure 3.14), where the azos adjacent to the NBEM retained a much more stable birefringence state than those adjacent to a styrene group. When considering these factors, and the inherent mobility in poly(electrolyte) multilayers, it is not too surprising that a stable birefringence was not noticed.

Figure 3.14 The structures of A) NBEM and B) Styrene. The steric factors associated with NBEN promote stability in birefringence compared to styrene

The birefringence was also examined at increasing humidities to see what role, if any, humidity had on birefringence. The same humidity cell as used for quantum yields was also used for birefringence experiments. The birefringence was not found to be stable at any humidity measured, however, a biexponential fit was made to each curve for both the growth (eq.16) and relaxation processes (eq.17). At 100% humidity, the decay could not be fit to a biexponential.

$$y = y0 + A1*(1 - \exp(-x/t1)) + B*(1 - \exp(-x/t2))$$
(16)

$$y = y0 + C*exp(-(x)/t3) + D*exp(-(x)/t4)$$
(17)

There were no apparent trends in the biexponential rise, or with regards to C and D, the weighting of the contributions of the biexponential decay curve with increasing humidity (Table 3.1).

Humidity (RH)	A	t1 (1/s)	В	t2(1/s)	C	t3(1/s)	D	t4(1/s)
0	0.51	0.077519	0.49	0.243902	0.50	0.1	0.50	0.013333
10	0.72	0.028571	0.28	0.131579	0.88	0.2	0.12	0.009009
40	0.59	0.066225	0.41	0.454545	0.57	0.083333	0.43	0.004608
60	0.44	0.208333	0.56	0.232558	0.72	0.058824	0.28	0.002398
78	0.50	0.0625	0.50	0.166667	0.56	0.1	0.44	0.002058
100	0.49	0.147059	0.51	0.16129				

Table 3.1 Parameters obtained by fitting the birefringence growth and decay curves to equations (1) and (2) respectively.

However, something interesting was noticed for the two rates contributing to the biexponential. The comparatively faster rate (t3) stayed relatively constant whereas the slower rate (t4) decreased noticeably with increasing humidity (Figure 4.7). An increase in humidity has been known to decrease relaxation rates, suggesting that perhaps t4 is due to *cis* to *trans* relaxation. However, it is also possible that the interaction with water could also change the rate for the molecules to randomize. Therefore, it cannot be determined yet which rate, fast or slow, accounts for which process.

The change of Relaxation Times t3 and t4 with Humidity

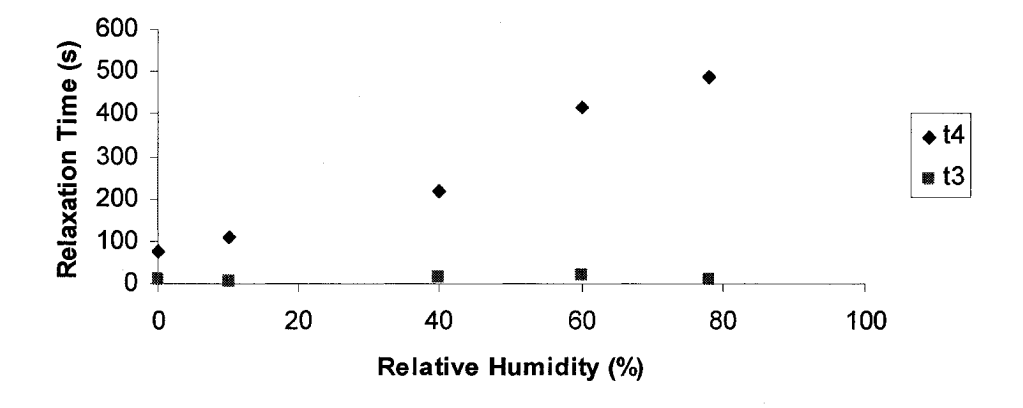


Figure 3.15 An increase in relaxation times, hence a decrease in relaxation rates, is seen with increased humidity for t4, the slower rate constant, whereas t3, the faster rate, stays relatively constant.

3.7 References

- [1] Dai, J.; Jensen, A.W.; Mohanty, D.K.; Erndt, J.; Bruening, M. L. *Langmuir* **2001**, *17*, 931.
- [2] Chung, A.J.; Rubner, M.F. Langmuir 2002, 18, 1176.
- [3] Tanchak, O.M.; Barrett, C.J. Chem. Mater. 2004, 16, 2734.
- [4] Tanchak, O.M.; Yager, K.G.; Fritzsche, H.; Harroun, T.; Katsaras, J.; Barrett, C.J. Langmuir 2006, 22, 5137.
- [5] Loucif-Saibi, R.; Nakatani, K.; Delaire, A.; Sekkat, Z.; Dumont, M. Chem. Mater. 1993, 5, 229.
- [6] Fischer, E. J. Phys. Chem. 1967, 71, 3704.
- [7] Rau, H.; Greiner, G. J. Phys. Chem. 1990, 94, 6523.
- [8] Ichimura, K. Chem. Rev. 2000, 100, 1847.
- [9] Torodov, T.; Nikolova, L.; Tomova, N. Appl. Opt. 1984, 23, 4309.
- [10] Ho, M.-S.; Natansohn, A.; Barrett, C.; Rochon, P. Can. J. Chem. 1995, 73, 1773.
- [11] Ho, M.-S.; Natansohn, A.; Rochon, P. Macromolecules 1995, 28, 6124.
- [12] Natansohn, A.; Rochon, P.; Xie, S. Macromolecules 1992, 25, 5531.
- [13] Meng, X.; Natansohn, A.; Rochon, P. J. Polym. Sci. Part B Polym. Phys. 1996, 34, 1461.
- [14] Iftime, G.; Fisher, L.; Natansohn, A.; Rochon, P. Can. J. Chem. 2000, 78, 409.
- [15] Nakamura O.; Ogino, I.; Kodama T. Rev. Sci. Instrum. 1979, 50, 1313.
- [16] Chang, M.-J.; Myerson, A.S.; Kwei, T.K. J. Appl. Polym. Sci. 1997, 66, 279.

- [17] Lamarre, L.; Sung C.S.P. Macromolecules 1983, 16, 1729.
- [18] Eisenbach, C. D. Macromol. Chem. 1978, 179, 2489.
- [19] Paik, C.S.; Morawetz, H. Macromolecules 1972, 5, 171.
- [20] Tsutsumi, N.; Yoshizaki, S.; Sakai, W.; Kiyotsukuri, T. Mol. Cryst. Liq. Cryst. Sci. Technol., Sect. B 1996, 15, 387.
- [21] Ahluwalia, A.; Piolanti, R.; De Rossi, D.; Fissi, A. Langmuir 1997, 13, 5909.

Supporting Information

Quantum Yield Variation with Humidity for 10 Layer Sample

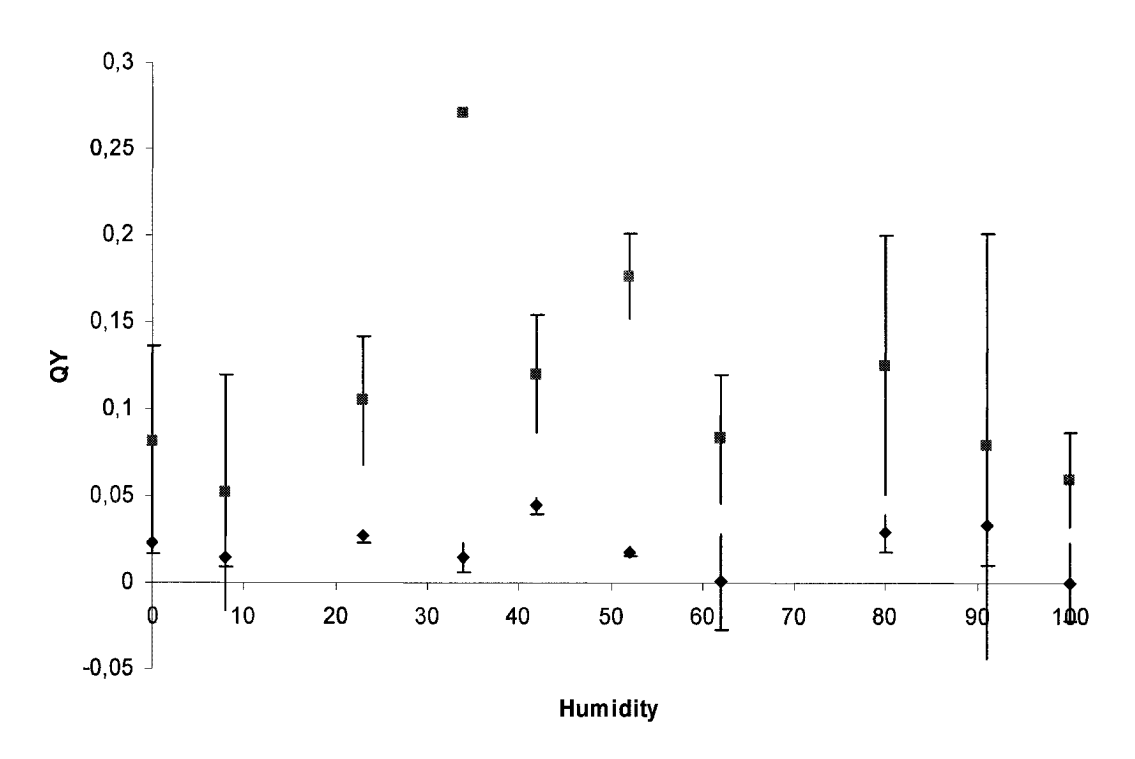
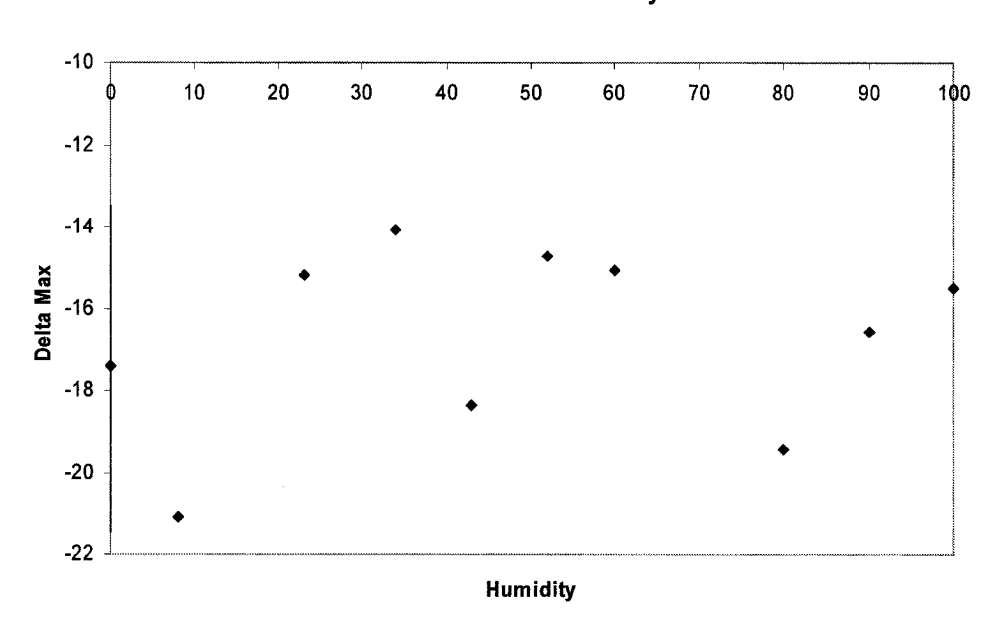
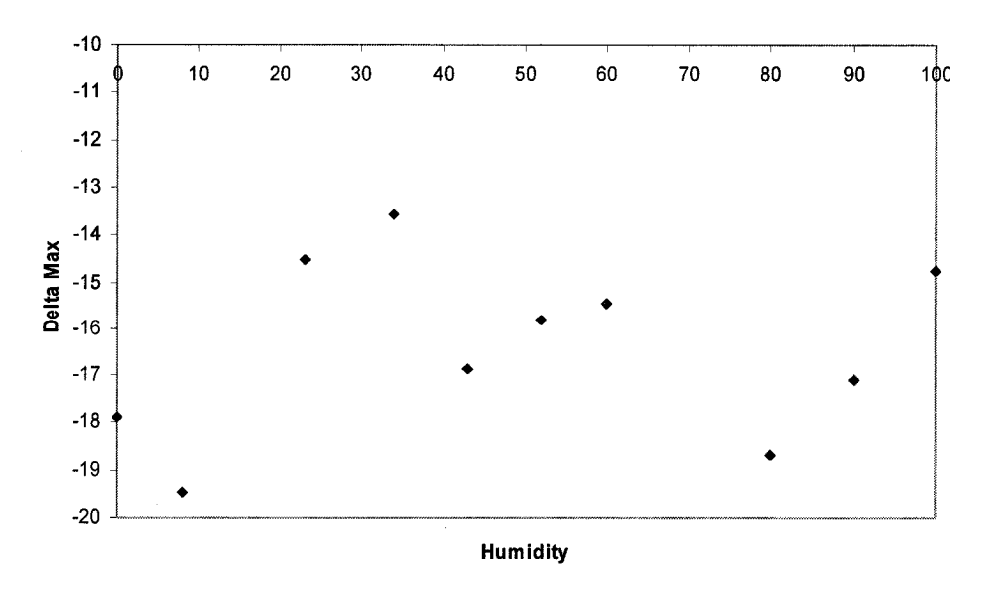


Figure 3.1S A similar trend was also seen with a 10-layer sample of PDR2. The error bars at 30% RH were too large to be shown.

Variation of Delta Max with Humidity -488-488



488-514 Delta Max Variations with Humidity



Variation of Delta Max with Humidity 514-514

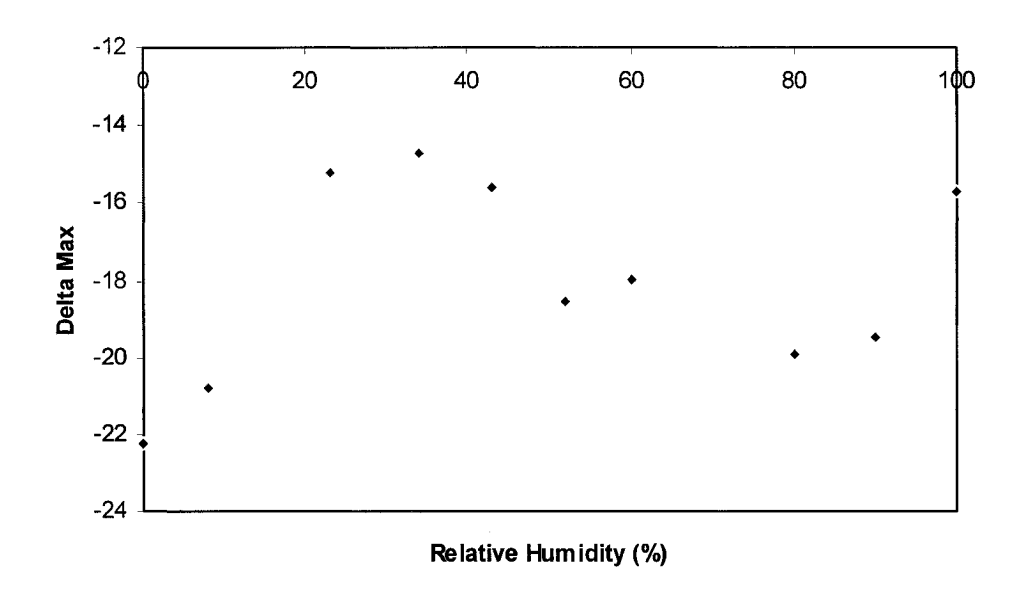


Figure 3.2S The variation with Δ max with humidity for each set of trials: 1) 488-488 pump-probe; 2) 514-488 pump-probe and 3) 514-514 pump-probe. This is the raw data of pump-probe experiments at increasing humidity extrapolated to infinity.

Chapter 4

CONCLUSIONS AND FUTURE WORK

4.1 Conclusions

This goal of this thesis was to create a photo-responsive, water-soluble azo polymer suitable for guiding neuron growth, and to characterize its physical and chemical properties. A new polymer, Disperse Red 2 (DR2), was synthesized and extensively characterized, and physical properties of DR2, including photochemical relaxation times, quantum yields, and birefringence, were investigated spectroscopically. Furthermore, the influence of humidity on physical properties was investigated. Chapter 1 provided an in-depth background of azobenzene systems, and in particular, azo polymers. Of particular interest were photochemical and photophysical parameters associated with the reversible trans to cis isomerization. Chapter 1 also described methods for synthesizing polymers and creating polymeric thin films along with potential applications for these materials.

Chapter 2 discussed possible synthetic routes for the creation of PDR2. It was found that the best method involved replacing the hydroxyl group on DR1 with an amine and reacting this with a polymer. Poly(acrylic acid), when reacted with oxalyl chloride to form an acyl chloride was found to be the best polymer to react with DR2. Characterization was performed using Nuclear Magnetic Resonance, Thermogravimetric Analysis, and Differential Scanning Calorimetry. The molar

extinction coefficient was also determined using ellipsometry to determine the thickness of the thin films and Ultra Violet Visible Spectroscopy to determine the absorbance.

Chapter 3 provided the background and method to calculate quantum yields and birefringence, along with the optical setups used. Quantum yields and birefringence were then calculated and their reliance on humidity was examined. Quantum yields for the trans to cis isomerization were found to be lower than quantum yields for the cis to trans reconversion. Quantum yields were found to increase with humidity until a maximum was attained at approximately 30 % humidity, at which point they decreased with increasing humidity. The original increase is explained by increased plasticization of the polymer matrix as water acts as a lubricant. The subsequent decrease in quantum yields is due to a combined effect water molecules creating a more polar environment inside the polymer matrix, resulting in a lowering of relaxation rates, and also to water clusters hindering the trans to cis isomerization. A stable birefringence state was not achieved for PDR2. This was due to a combination of low azo content in the polymer, the inherent mobility of polyelectrolyte multilayers (PEMs), and a lack of interaction with the poly(acrylic acid) backbone. Two processes, a fast rate and slow rate, contributing to the biexponential birefringence relaxation were cis to trans relaxation, and dipole interactions between side groups. The faster rate stayed relatively constant with increased humidity, whereas the slower decreased substantially. It could not be

determined which process was accounted for which rate, as both processes could be affected by humidity.

4.2 Future Work

A novel water-soluble molecule was created using DR1 and poly(acrylic acid) as the basic component materials. The synthetic route used could be adjusted to allow for different types of photoresponsive compounds other than DR2, or the backbone could be modified to explore what changes, if any, the backbone would induce. Gel Permeation Chromatography was unable to disclose any information about the molecular weight of the polymer due to the low molecular weight of the poly(acrylic acid) backbone, so creating the molecule with a higher molecular weight polymer should be performed. This thesis showed that humidity affects both quantum yields and birefringence, and that compounds are most photoefficient at moderate humidity. Factors such as azo content, or the pH used for assembly could also be investigated as variables to further enhance quantum yields. A more in-depth study on birefringence could be performed. This thesis claimed that a stable birefringence state could not be achieved due to azo content, and also to the mobility of PEMs. This claim could be tested by creating PDR2 with azo content of at least 20% to ensure that a stable birefringence state can be achieved with high enough chromophore.

Finally, the original purpose of this project was to create novel materials used for guiding neuron growth. These materials provide a surface for neurons to grow, and by exploiting the changes that occur upon photoisomeirzation, both physically and chemically, to enhance the differences between favourable and unfavourable growth media, the optical guided growth of neurons could be achieved.